Circulation Research
JOURNAL OF THE AMERICAN HEART ASSOCIATION

American Heart Association®
Learn and Live℠

Erythropoietin-Mobilized Endothelial Progenitors Enhance Reendothelialization via Akt-Endothelial Nitric Oxide Synthase Activation and Prevent Neointimal Hyperplasia

Norifumi Urao, Mitsuhiko Okigaki, Hiroyuki Yamada, Yasushi Aadachi, Kuniharu Matsuno, Akihiro Matsui, Shinsaku Matsunaga, Kento Tateishi, Tetsuya Nomura, Tomosaburo Takahashi, Tetsuya Tatsumi and Hiroaki Matsubara

Circ. Res. 2006;98;1405-1413; originally published online Apr 27, 2006;
DOI: 10.1161/01.RES.0000224117.59417.f3
Circulation Research is published by the American Heart Association. 7272 Greenville Avenue, Dallas, TX 72514
 Print ISSN: 0009-7330. Online ISSN: 1524-4571

Erythropoietin-Mobilized Endothelial Progenitors Enhance Reendothelialization via Akt–Endothelial Nitric Oxide Synthase Activation and Prevent Neointimal Hyperplasia

Norifumi Urao, Mitsuhiko Okigaki, Hiroyuki Yamada, Yasushi Aadachi, Kuniharu Matsuno, Akihiro Matsui, Shinsaku Matsunaga, Kento Tateishi, Tetsuya Nomura, Tomosaburo Takahashi, Tetsuya Tatsumi, Hiroaki Matsubara

Abstract—We investigated whether the mobilization of endothelial progenitor cells (EPCs) by exogenous erythropoietin (Epo) promotes the repair of injured endothelium. Recombinant human Epo was injected (1000 IU/kg for the initial 3 days) after wire injury of the femoral artery of mice. Neointimal formation was inhibited by Epo to 48% of the control ($P<0.05$) in an NO-dependent manner. Epo induced a 1.4-fold increase in reendothelialized area of day 14 denuded vessels, 55% of which was derived from bone marrow (BM) cells. Epo increased the circulating Sca-1^+/Flk-1^+ EPCs (2.0-fold, $P<0.05$) with endothelial properties NO dependently. BM replacement by GFP- or β-galactosidase–overexpressing cells showed that Epo stimulated both differentiation of BM-derived EPCs and proliferation of resident ECs. BM-derived ECs increased 2.2- to 2.7-fold ($P<0.05$) in the Epo-induced neoendothelium, where the expression of Epo receptor was upregulated. Epo induced Akt/eNOS phosphorylation and NO synthesis on EPCs and exerted an antiapoptotic action on wire-injured arteries. In conclusion, Epo treatment inhibits the neointimal hyperplasia after arterial injury in an NO-dependent manner by acting on the injured vessels and mobilizing EPCs to the neo-endothelium. **(*Circ Res*. 2006;98:1405-1413.)**

Key Words: restenosis ■ endothelium ■ progenitor cells ■ erythropoietin

Endothelial cells (ECs) cover the luminal surface of blood vessels and maintain multiple vascular functions. Disruption of endothelial coverage causes a decrease in the production of vasculoprotective mediators such as nitric oxide (NO), leading to elevated vascular tonus, enhanced inflammation and medial smooth muscle cell proliferation. The resultant neointimal hyperplasia causes restenosis in various pathological conditions.[1]

Bone marrow (BM)-derived endothelial progenitor cells (EPCs) have been isolated from the mononuclear cell (MNC) population in peripheral blood (PB).[2,3] They have differentiated into ECs,[2] suggesting that they may have a potential to accelerate reendothelialization. Recently, transplantation of autologous PB EPCs to balloon-denuded arteries was reported to facilitate reendothelialization of the injured artery.[4,5] Intravenous transfusion of spleen-derived EPCs or EPCs overexpressing eNOS reduces neointimal formation after vascular injury.[6,7] Delivery of primary cultured PB MNCs to balloon-injured arteries leads to accelerated reendothelialization to promote endothelium-dependent vasoreactivity.[8]

Erythropoietin (Epo) stimulates the proliferation and differentiation of erythroid lineage progenitors. Mature ECs express Epo receptors (EpoRs),[9] and Epo induces proangiogenic response in cultivated mature ECs, as evidenced by EC proliferation and migration[10] and the antiapoptotic effect on ECs[11] as well as NO production.[12] Epo increases circulating EPCs to stimulate neovascularization in vivo[13] or induces proangiogenic phenotype in cultured ECs[14] and also improves wound healing by angiogenesis in the genetically diabetic mouse.[15] This evidence leads to the hypothesis that Epo may provide an effective noninvasive strategy to enhance reendothelialization of injured vessels.

Several studies have shown that the exogenous administration of cytokines increases the number of circulating EPCs. For example, pretreatment with vascular endothelial growth factor (VEGF) was reported to double the number of circulating EPCs in humans,[16,17] and the administration of granulocyte colony–stimulating factor (G-CSF) recruited EPCs from BM.[17] Mobilization of the circulating EPCs by exogenous G-CSF facilitates reendothelialization and inhibits neointimal development.[18]

In this study, we evaluated the efficacy of short-term Epo treatment as a strategy for promoting reendothelialization followed by the inhibition of neointimal hyperplasia in

Original received November 28, 2005; revision received March 22, 2006; accepted April 18, 2006.

From the Departments of Cardiovascular Medicine (N.U., M.O., H.Y., A.M., S.M., K.T., T.N., T. Takahashi, T. Tatsumi, H.M.) and Pharmacology (K.M.), Kyoto Prefectural University of Medicine; and Department of Pathology (Y.A.), Kansai Medical University, Osaka, Japan.

Correspondence to Mitsuhiko Okigaki, MD, Department of Cardiovascular Medicine, Kyoto Prefectural University of Medicine, Kamigyo-ku, Kyoto 602-8566, Japan. E-mail okigakim@koto.kpu-m.ac.jp

Circulation Research **is available at http://circres.ahajournals.org** **DOI: 10.1161/01.RES.0000224117.59417.f3**

wire-injured arteries. Our results show that only 3-day treatment with Epo causes mobilization of circulating $CD45^{dim}$/Flk-1^+ or Sca1^+/Flk-1^+ EPCs and stimulates both differentiation of BM-derived EPCs on the endothelial layer and proliferation of resident ECs associated with endothelial EpoR-mediated activation of the Akt-eNOS pathway and SMC antiapoptotic effect, resulting in a marked inhibition of neointimal formation.

Materials and Methods

Vascular Injury, Epo Administration, and Morphometric Analysis

Transluminal arterial injury was performed in 8-week-old male C57BL/6 mice. A straight spring wire (0.25 mm in diameter) was inserted into the left femoral artery and placed there for 3 minutes. This wire injury was reported to cause a complete removal of endothelium.[19] Human Epo (Chugai, Tokyo) (1000 IU/kg body weight) or saline was injected intraperitoneally just after arterial injury and once daily for the following 2 days. Treatment with N^G-nitro-L-arginine methyl ester (L-NAME) (3.7 mmol/L) or 2.25% L-arginine hydrochloride (106.8 mmol/L; Sigma) in the drinking water took place for 7 days before wire injury and continued for 14 days after wire injury.

The dose of Epo was determined based on the previous report.[13] The injured arteries were harvested at day 14 and fixed with 4% paraformaldehyde. Paraffin-embedded sections were stained with Elastica van Gieson. Three sections from each artery at 300-μm intervals were analyzed using ImageJ 1.32j software (NIH). In other animals, Evans blue dye (5%; Sigma) was transfused to mice 10 minutes before euthanasia to identify the remaining denuded area 5 and 14 days after wire injury. After removal, arterial tissues were longitudinally opened and then placed on slide glasses to take pictures under microscope (MS5 Olympus). All animal procedures were approved by institutional guidelines. The collection of blood samples and the consent protocol for the volunters was approved by institutional guidelines.

Fluorescence-Activated Cell Sorting

PB (100 μL) was collected 3 days after injury and incubated for 15 minutes with anti-mouse CD34–fluorescein isothiocyanate (FITC), Flk-1-PE, Sca1-FITC, CD45-PECy5 antibodies (BD Pharmingen). After erythrocyte lysis, cells were analyzed with FACS Caliber (Becton Dickinson). $CD45^{dim}$/Flk-1^+ cells and Sca1^+/Flk-1^+ cells were sorted with FACS Vantage to give a culture assay and RT-PCR analysis, respectively.

Murine Cell Culture Assay

The sorted $CD45^{dim}$/Flk-1^+ cells were cultured with EBM-2 medium supplemented with 5% FBS, EGM-2-MV-SingleQuots (Clonetics), and 10 ng/mL VEGF (Peprotech) on fibronectin-coated chamber slides (Becton Dickinson). Adherent cells were reseeded after 4 days and maintained for 7 days. The culture cells were incubated with 2.4 μL/mL Alexa Fluor 594-labeled acetylated LDL (acLDL) (Molecular Probes) for 120 minutes, fixed with 2% paraformaldehyde, and incubated with 10 ng/mL of BS-1-FITC (Sigma) for 1 hour, and double-fluorescent cells were counted as EPCs in 4 randomly selected fields under confocal microscopy (FLUOVIEW BX50; Olympus).

Immunohistochemistry

Arteries were harvested on day 14 and fixed in 4% paraformaldehyde. Paraffin cross-sections were stained with antibodies against CD31 (sc-8306; Santa Cruz Biotechnology) and EpoR (sc-5624 or sc-697) followed by the avidin–biotin complex technique and diaminobenzidine substrate (Vector Laboratories). Sections were counterstained with hematoxylin. Frozen sections were stained with antibodies (GFP-Alexa Fluor 488, Molecular Probes; CD31-PE, BD Pharmingen), followed by Alexa Fluor 633–conjugated anti-rabbit IgG secondary antibody (Molecular Probes), and then observed under the confocal microscopy. The number of fluorescent cells from 6 sections was evaluated statistically.

To detect apoptotic cells in situ, TdT-mediated dUTP-biotin nick end labeling (TUNEL) staining was performed for paraffin sections using the In-Situ Cell Death Detection Kit (Chemicon International Inc) and counterstained with methyl green.

BM Transplantation

GFP transgenic mice were generously provided from Dr Okabe (Osaka University).[20] ROSA mice[21] were purchased from The Jackson Laboratory (Bar Harbor, Me). GFP- or β-galactosidase–overexpressing BM cells (5×10^6) were transfused to recipient mice 24 hours after 9 Gray irradiation. Six weeks after transplantation, they were subjected to vascular injury. Subsequently, at day 14 after injury, mice were examined.

Human Cell Isolation and Culture

PB was obtained. PB MNCs from venous blood of healthy human volunteers were isolated by density-gradient centrifugation (Lymphoprep; Axis Shield). $CD133^+$ progenitor cells were purified from PB MNCs by positive selection with anti-$CD133^+$ microbeads respectively using magnetic cell sorter device (Miltenyi Biotec). The purity of sorted cells assessed by fluorescence-activated cell sorter (FACS) analysis was grater than 90%. The $CD133^+$ progenitor cells were cultured in EBM-2 medium supplemented with 5% FBS, EGM-2-MV-SingleQuots (Clonetics) a day before analysis, as described below. All cells were maintained at 37°C in a humidified incubator at 5% CO_2. After serum starved in DMEM supplemented with 0.5% FBS for 12 hours, they were stimulated with 1.2IU/mL of Epo for 30 minutes and fixed. Immunofluorescence was performed by using antibodies against EpoR (sc-5624; Santa Cruz Biotechnology) with phosphorylated Akt and eNOS (Cell Signaling Technology). For double staining, we used Zenon rabbit IgG labeling kits (Molecular Probes) only when needed.

For measurement of the intracellular NO level, the cells were loaded with 4-amino-5-methylamino-2′,7′-difluorofluorescein diacetate (DAF-FM DA) (10 μmol/L; Daiichi Pure Chemicals, Tokyo, Japan) for 30 minutes at 37°C in the dark, washed twice with buffer, incubated for another 30 minutes, and then visualized under laser microscopy.

Fluorescent intensity was evaluated with Adobe Photoshop software.

Measurement of NOx Concentration

NOx concentration in the serum was measured with a high-performance liquid chromatography (HPLC) Griess system, as previously described.[22]

Statistics

Statistical analyses were performed with 1-way ANOVA followed by pair-wise contrasts using the Dunnett's test. Data are expressed as means±SE for continuous variables. $P<0.05$ was considered statistically significant.

Results

Epo Inhibits Neointimal Hyperplasia

A prominent, concentric neointima developed in the saline-treated vessels 14 days after injury, whereas neointimal formation was markedly reduced in the Epo-treated animals (Figure 1A). Morphometric analysis of serial sections (Figure 1B) showed a marked decrease (52%, n=10, $P<0.05$) in the neointimal area in the Epo-treated mice compared with the saline-injected group. The ratio of intima to medial area (I/M ratio) in the Epo-treated mice was significantly smaller (46%, n=10, $P<0.05$) than that in the saline-treated mice, whereas

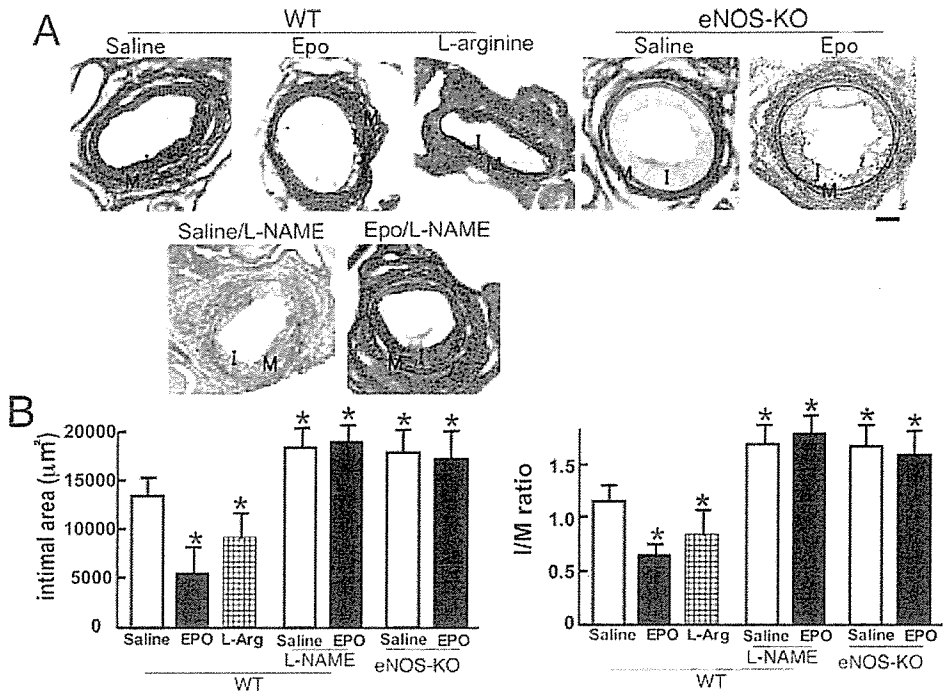

Figure 1. Epo-mediated inhibition of neointimal hyperplasia in NO-dependent manner. The wild-type or eNOS-null mice were subjected to the wire injury of femoral arteries and then treated with Epo or saline for the initial 3 days. Treatment with L-NAME (3.7 mmol/L) or 2.25% L-arginine hydrochloride (106.8 mmol/L) in the drinking water was started 7 days before wire injury and continued for 14 days until arterial sampling. A, Elastica van Gieson–stained sections on day 14. Scale bar=100 μm. I indicates intima; M, media. B, Quantification of the neointimal area and the I/M ratio averaged on 3 different sections of each artery (n=10 each). *$P<0.05$ vs saline-treated wild-type mice.

medial thickness did not significantly differ between either group (data not shown).

As the involvement of NO in the neointimal hyperplasia has been reported,[23] we next examined the effect of L-NAME on the Epo-mediated inhibition. Seven-day pretreatment with L-NAME significantly aggravated the neointimal hyperplasia in the saline-treated control mice (31%, n=10, $P<0.05$), consistent with the previous reports using eNOS-null mice.[24] Interestingly, L-NAME completely abolished Epo-mediated inhibitory effect on the neointimal hyperplasia (I/M ratio;1.61±0.38 versus 0.63±0.15 in the Epo-treat mice, $P<0.05$, n=10 each) (Figure 1A and 1B), suggesting the involvement of NO in Epo-mediated action. Furthermore, treatment with the NO donor L-arginine reduced the neointimal area to the level comparable to the Epo-treated mice (Figure 1A and 1B).

To confirm that the Epo-mediated inhibition of the neointimal formation is eNOS/NO dependent, we performed the arterial injury in the eNOS-null mice. The neointimal formation in the Epo-treated eNOS-null mice was aggravated (2.8-fold, n=7, $P<0.005$) compared with that of the Epo-treated wild-type mice, which was similar to the level in the Epo plus L-NAME–treated mice (2.9-fold, n=10, $P<0.005$) (Figure 1A and 1B).

The hemoglobin value was significantly higher after Epo treatment than that of the saline-treated controls (12.6±0.4 versus 14.0±0.1 g/dL at day 9, n=15, $P<0.05$). The number of white blood cells reached a peak on day 2 in both groups and was significantly higher in the Epo-treated mice (18 600±2020 versus 10 200±1100 cells/μL of control, n=15, $P<0.05$). The platelet number was similar in both groups on days 2 and 9.

Epo Promotes Reendothelialization

Evans blue dye was administered premortem to stain the nonendothelialized areas 5 and 14 days after injury. Nonendothelialized lesions are marked by blue staining, whereas the reendothelialized area appears white (Figure 2A). At both time points, the reendothelialized area in the Epo-treated group was significantly larger than that in the saline-treated group (1.4- and 1.8-fold on day 5 and -14, n=6, respectively) (Figure 2A). Immunostaining with anti-CD31 antibody in transverse sections revealed that the proportion of $CD31^+$ length to total lumen surface was 1.4-fold greater in the Epo-treated mice (n=10, $P<0.05$) (Figure 2B), consistent with the result from Evans Blue dye experiment. Furthermore, the NO dependency of the Epo-promoted reendothelialization was evaluated. The $CD31^+$ endothelial area in the total lumen length in the Epo plus L-NAME–treated mice was 65% lower than that in the Epo-treated mice (n=10, $P<0.01$) and similar to the saline-treated control mice (Figure 2B).

Epo Facilitates Mobilization of EPCs

$CD45^{dim}$ cells were gated from PB MNCs and subsequently analyzed for the expression of endothelial lineage markers, Flk-1 and CD34. Three-day Epo treatment mobilized the $CD45^{dim}$ cells into circulation (Figure 3A), and the ratio of $CD45^{dim}/Flk\text{-}1^+$ cells to total PB MNCs increased to 7.4-fold (n=5 each, $P<0.05$) (Figure 3A, right). We further investi-

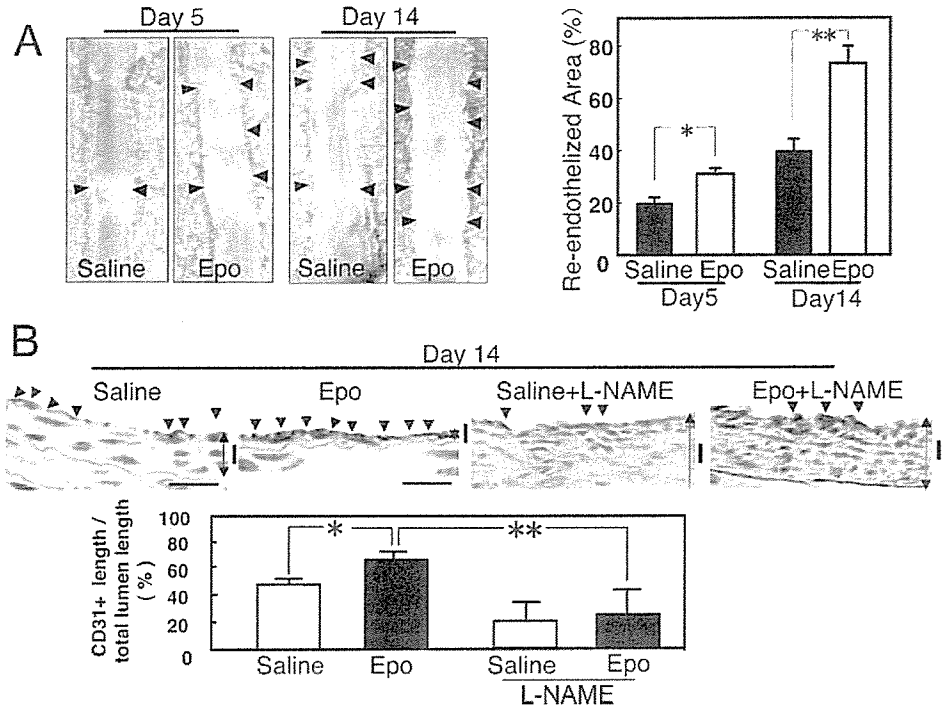

Figure 2. Epo facilitated reendothelialization after wire injury. A, Evans blue dye was injected 10 minutes before euthanasia on days 5 and 14. Nonendothelialized lesions are marked by blue staining, whereas the reendothelialized area appears white (arrowhead). Quantification of the reendothelialized areas was performed with computed morphometry (n=6 each, $^{*}P<0.01$, $^{**}P=0.02$). B, Fourteen days after arterial injury with and without L-NAME pretreatment, the lesion was subjected to histological analysis. ECs were identified by immunostaining with anti-CD31 antibody in day-14 artery samples. Apparent $CD31^{+}$ area is indicated by arrowheads. The ratio of $CD31^{+}$ length to lumen perimeter in sections were evaluated and averaged on 5 different cross-sections from each artery (n=10, $^{*}P<0.05$, $^{**}P<0.01$). I indicates intima.

gated the effect of L-NAME pretreatment on the Epo-mediated mobilization of EPCs using anti-Sca1 and anti–Flk-1 antibodies. The number of circulating $Sca1^{+}/Flk\text{-}1^{+}$ cells in the control group was markedly increased than the basal level (2-fold, n=6, $P<0.05$), whereas in the L-NAME–treated group, the Epo-mediated mobilization was completely inhibited (Figure 3B).

To confirm the endothelial property of $CD45^{dim}/Flk\text{-}1^{+}$ cells, we cultured them for 7 days in EGM medium with 10 ng/mL VEGF, and the EC-specific function was examined. Confocal microscopy demonstrated that 93±5% of cultured $CD45^{dim}/Flk\text{-}1^{+}$ cells were bound to FITC-conjugated BS-1 lectin and incorporated DiI-labeled acLDL, a commonly used identifier of endothelial lineage cells (Figure 3C). To evaluate the number of circulating EPCs, PB MNCs were isolated 3 days after Epo or saline treatment and cultured for 7 days. The relative numbers of BS-1 $lectin^{+}/acLDL^{+}$ cells from Epo-treated mice were 5.2±0.5-fold higher (n=5, $P<0.02$) than that in the saline-injected control (Figure 3D).

Antiapoptotic Effect on Medial SMC After Vascular Wire Injury

The procedure of wire injury of mouse femoral artery causes complete removal of endothelium, resulting in rapid apoptosis of medial SMCs that enhances neointimal hyperplasia.[19,25] Inhibition of this burst apoptosis is reported to be a preventive effect on neointimal hyperplasia.[26] Figure 3E shows that at 2 and 4 hours after injury, the number of TUNEL-positive apoptotic cells in the Epo-treated artery was significantly ($P<0.05$) decreased to 25% and 39% of the saline-treated controls, respectively. L-NAME treatment did not affect the Epo-mediated protection of VSMC apoptosis. Considering that the endothelium was completely removed by wire injury and the expression of EpoR in the EC-denuded artery was detected by RT-PCR analysis (unpublished observation, 2006), these findings suggest that Epo directly affects the apoptosis of VSMCs after wire injury. Interestingly, at 6 hours after injury, the number of apoptotic cell in the Epo-treated mice was increased to the level similar to the saline-treated mice, suggesting that Epo treatment did not prevent, but shifted, the apoptosis of VSMCs after wire injury.

The biological effects of Epo in the injured artery may be attributable to Epo-induced increase in circulating NO pool produced by the remote endothelial cells. Plasma NOx concentrations at 1, 2, 4, and 6 hours and 1, 3, and 14 days after injury of the Epo-treated mice were similar to those of the control mice (day 1: 54.3±8.6 versus 57.2±9.7; day 3: 58.6±9.6 versus 55.3±10.2; day 14: 59.6±4.6 versus 60.8±6.5 μmol/L; n=7 each). The expression levels for eNOS and EpoR in the lung and carotid artery at the same time points were comparable with the control mice when assessed by Western blotting and RT-PCR analysis, respectively (data not shown). These findings suggest that Epo-

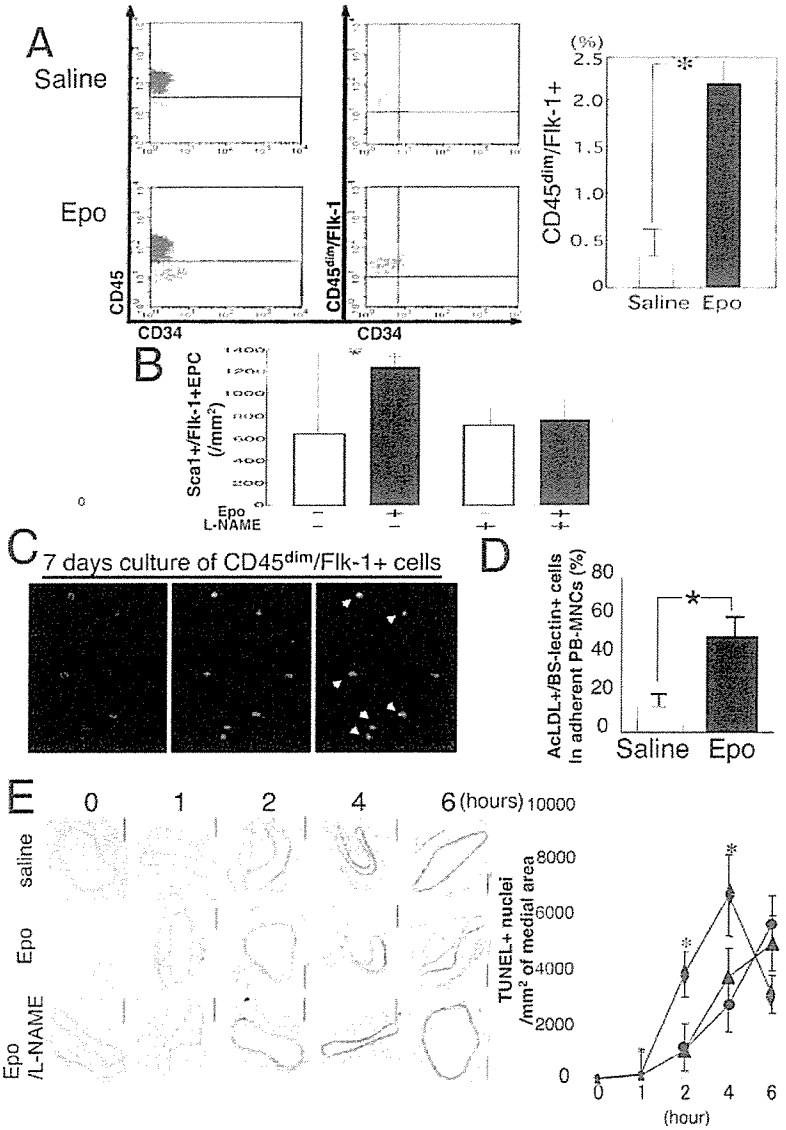

Figure 3. Identification of Epo-mobilized endothelial progenitor cells and antiapoptotic effect on medial SMCs. A, PB was collected 3 days after injury and subjected to FACS analysis. $CD45^{dim}$ cells were gated and subsequently analyzed for Flk-1 and CD34 expression. Right, Percentage of the $CD45^{dim}/Flk\text{-}1^+$ cells in total PB MNCs was higher in the Epo-treated group (n=5, $^*P<0.05$). B, Evaluation of the number of circulating $Sca1^+/Flk\text{-}1^+$ EPCs by FACS analysis. After 3 days of Epo treatment, the number of the circulating $Sca1^+/Flk\text{-}1^+$ EPCs per millimeter squared of PB of the mice with or without 7 days of L-NAME pretreatment was evaluated ($^*P<0.05$, each n=4). C, Differentiation of $CD45^{dim}/Flk\text{-}1^+$ cells into endothelial-lineage cells. PB MNCs were prepared from the 3-day Epo-treated mice, $CD45^{dim}/Flk\text{-}1^+$ cells were sorted and primarily cultured for 7 days, and the endothelial properties were examined by the uptake of DiI-acLDL and binding to FITC–BS-1 lectin. Cells in the merged image (right, arrowheads) indicate BS-1 $lectin^+/acLDL^+$ double-fluorescent cells. D, Total PB MNCs were primary cultured in endothelial medium for 7 days. The ratio of adherent cells with BS-1 $lectin^+/acLDL^+$ EC-like property was shown (n=5, $^*P<0.02$). E, Time course of the apoptosis in the injured artery. Femoral arteries of mice treated with Epo, Epo plus L-NAME, or saline (n=5 each) were analyzed before and after 1, 2, 4, and 6 hours after wire injury. Apoptotic nuclei were detected as brown dots by TUNEL staining. Right, Semiquantification of $TUNEL^+$ nuclei in the medial area. Diamond, circle, and triangle indicate saline-, Epo-, and Epo plus L-NAME–treated mice, respectively. $^*P<0.05$ vs to Epo- and Epo plus L-NAME–treated mice.

mediated action unlikely results from the nonspecific increase in circulating NO pool.

Analysis by BM Replacement Model

We further examined whether Epo actually induces the incorporation of marrow-derived EPCs into the regenerated endothelium by transplanting GFP-overexpressing or β-galactosidase BM cells to the BM-ablated background mice. Six weeks after transplantation, 96±2% and 94±3% of PB MNCs were replaced, respectively (n=5 each; FACS data not shown). The mice that received vascular injury were examined on day 14. GFP^+ and $\beta\text{-}Gal^+$ cells were patchily detected in the endothelial layer, and double-fluorescence immunohistochemistry (Figure 4A and 4B) disclosed a significant increase in the $GFP^+/CD31^+$ and $\beta\text{-}Gal^+/CD31^+$ lesions (2.7- and 2.2-fold, respectively, $P<0.05$) in Epo-treated mice compared with the saline-treated mice (Figure 4A and 4B). The ratio of Epo-induced GFP^+ area in total $CD31^+$ regenerated endothelium was 31±0.3% (n=5) (Figure 4A), suggesting that Epo-mediated reendothelialization is composed of differentiation of BM-derived EPCs as well as facilitated proliferation of resident ECs. In addition, the numbers of BM-derived macrophages ($GFP^+/MOMA2^+$) and vascular smooth muscle cells ($GFP^+/\alpha SMA^+$) in the neointima of the Epo-treated mice were much lower than those of the control group (Figure 4A). $GFP^+/CD3^+$ or $GFP^+/B220^+$ cells were barely detectable in the neointima of both groups (data not shown).

Expression of EpoR in Epo-Treated Injured Artery

We investigated whether Epo-mobilized EPCs actually express the specific receptor for Epo (EpoR). EpoR-positive cells (brown staining, arrowheads in Figure 5A) were apparently localized on the regenerated endothelium in the Epo-treated arteries, whereas the expression of EpoR in the saline-treated injured or uninjured arteries was barely detectable.

The immunofluorescence study using anti-EpoR, anti-CD31, anti-CD45, and anti–αSM-actin (αSMA) antibodies revealed that $CD31^+$ endothelial cells in Epo-treated arteries coexpressed EpoR on the endothelial layer, whereas neither

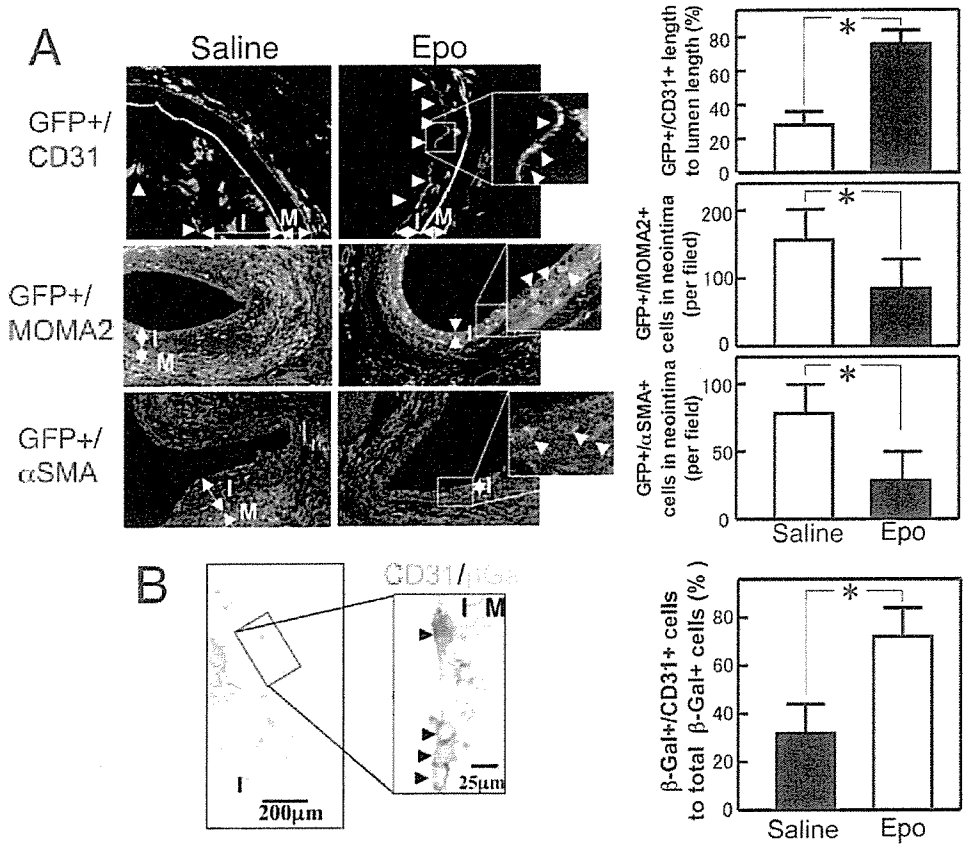

Figure 4. Incorporation of BM-derived cells into regenerated endothelium. A, BM cells from donor GFP–overexpressing mice were transfused to the irradiated recipient mice and subject to vascular injury. The day-14 samples were immunostained with antibodies against CD31, MOMA2, αSMA, and GFP. The localizations of double-fluorescent cells, including $GFP^+/CD31^+$, $GFP^+/MOMA2$, and $GFP^+/\alpha SMA$ cells, are shown as yellow dots in the merged image (arrowheads, bar=20 μm). Semiquantitative analysis of the double-fluorescent cell area per section is shown relative to the total lumen length or the number in the neointima (n=5 each, $^*P<0.02$). B, BM cells from donor β-Gal–overexpressing mice were transfused to the irradiated recipient mice and subjected to vascular injury. β-Gal–expressing cells (blue) and $CD31^+$ cells (brown) were observed in the day-14 samples. $\beta\text{-Gal}^+/CD31^+$ double-stained cells are indicated by arrowheads, and the relative ratio to total $\beta\text{-Gal}^+$ cells is shown (n=5 in each group, $^*P<0.05$).

$CD45^+$ cells nor αSMA^+ cells expressed EpoR (Figure 5B). We also confirmed the expression of EpoR in the BM-derived EC-like cells mobilized by Epo using the mice repopulated with GFP^+ BM cells (Figure 5C). Abundant $GFP^+/EpoR^+$ cells were detected on the luminal surface in the Epo-treated injured artery, and the distribution was 2.5-fold greater than that in the saline-treated mice ($P<0.05$, Figure 5D).

Epo Activates Akt-eNOS Pathways and NO Production in EPCs

To investigate whether PB and BM EPCs express EpoR, $Sca1^+/Flk\text{-}1^+$ EPCs were isolated from PB and BM by FACS and subjected to RT-PCR analysis. The DNA fragment corresponding to EpoR was amplified in the predicted size (Figure 6A). We further studied whether $Sca1^+/Flk\text{-}1^+$ EPCs have the ability to activate the EpoR/Akt/eNOS pathway in response to Epo treatment. Because the PB volume obtained from the mice is too little to get the sufficient number of endothelial-lineage cells attaching on the plate, and also the attaching mice-derived cells are less spreading and less proliferative compared with the human cells, we used the human PB EPCs. The $CD133^+$ EPCs were isolated from human PB by magnetic-associated cell sorting and primarily cultured. To study the stimulatory effect of Epo on the downstream pathway, after 12-hour serum starvation (0.5% serum), $CD133^+$ EPCs were treated with 1.2 IU/mL Epo for 30 minutes. Double staining using anti-EpoR with anti–phosphorylated Akt or anti–phosphorylated eNOS antibodies showed that Epo markedly induced Akt-eNOS phosphorylation in EpoR-positive EPCs (Figure 6B).

We further measured the intracellular NO level with DAF-FM DA (10 μmol/L). NO was visualized as a green dot under laser microscopy (Figure 6C). Epo stimulation upregulated NO level to 1.7-fold higher than the untreated control level ($P<0.05$), whereas addition of L-NAME completely abolished this increase.

Discussion

The balloon-mediated injury of endothelial integrity stimulates a regeneration of the EC monolayer, but this regenerative process is slow and cannot prevent the early proliferative events leading to the onset of a neointimal lesion. A novel approach that promotes early reendothelialization is required to potentiate this natural regenerative process. In this study, we examined whether Epo treatment is a feasible strategy to cause reendothelialization of wire-injured vessels. Our results

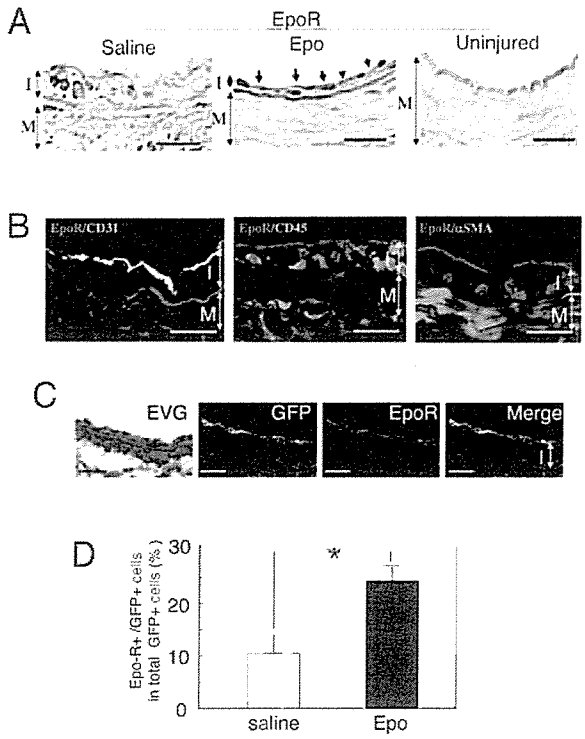

Figure 5. Localization and characterization of EpoR-expressing cells in neointima. A, Immunohistochemistry for EpoR showing the abundant localization of EpoR-expressing cells (brown, arrowheads) in the Epo-treated artery (day-14 sample) compared with saline-treated control and uninjured artery (bar=50 μm). B, Double-immunofluorescent images for EpoR (red) and CD31 (green, left), CD45 (green, middle), or αSMA (green, right) (bar=20 μm) showing coexpression of EpoR in $CD31^+$ cells. C, Localization of BM-derived EpoR-expressing cells in Epo-treated mice repopulated with GFP-overexpressing BM cells. Elastica van Gieson–stained sections (left) and immunofluorescent images for GFP (green) and EpoR (red) showing the localization of BM-derived $EpoR^+$ cells (yellow in merge image) along neointimal surface (bar=50 μm). D, Relative percentage of BM-derived EpoR-expressing cells in total BM-derived GFP^+ cells in the neointima (n=5 each, $^*P<0.05$). I indicates intima; M, media.

demonstrated that the 3-day treatment of Epo increases the circulating $Sca\text{-}1^+/Flk\text{-}1^+$ EPCs expressing an EpoR and that the mobilized EPCs contribute to the reendothelialization, leading to the inhibition of neointimal hyperplasia in an NO-dependent manner. Furthermore, we found that EpoR expression is upregulated in the Epo-induced neoendothelium and that the Epo/EpoR system causes the activation of the Akt-eNOS pathway on the EPCs and inhibits the apoptosis of medial SMCs.

EPCs can be harvested from PB, and intravenous transplantation of EPCs into EC-denuded vessels potentiates the recovery of endothelial integrity that causes the inhibition of neointimal hyperplasia,[4,8] although cell transplantation protocols, such as the ex vivo expansion of EPCs, are technically challenging. G-CSF–induced EPCs were shown to enhance the repair of injured arteries and prevent intimal hyperplasia.[18] However, it appears that the safety and feasibility of G-CSF treatment focusing on the induction of vascular occlusion in atherosclerotic lesions has not yet been established. In 12 intractable angina patients, the administration of G-CSF was associated with 2 cases of acute myocardial infarction and 1 case of cardiac death.[27] There are articles reporting the induction of acute myocardial infarction and cerebral infarction in G-CSF–treated BM transplantation patients.[28,29] Differentiation of G-CSF–mobilized progenitor cells into VSMC within the stented segment, induction of angiogenesis within the atherosclerotic lesion, and aggregation of mobilized inflammatory cells within the plaque may be plausible explanations.

This study showed that short-term (3-day) treatment with Epo after EC-denuded injury leads to accelerated reendothelialization and marked inhibition of neointimal formation. Figure 2A demonstrates that the ratio of reendothelialization by Epo and saline treatment is 73% and 41% on the total lumen area, respectively, whereas the coverage by $CD31^+$ marrow-derived cells on the reendothelialized lumen area is 75% and 32%, respectively (Figure 4B), indicating that 55% of Epo-mediated reendothelialized area is derived from marrow cells, and, in the saline-treated control, 13% of reendothelialized area is marrow-derived cells. Considering that Epo-mediated EPC mobilization (Figure 3) and reendothelialization (Figure 2) are NO dependent, it is suggested that EPC release via Epo and the endothelial differentiation in the repair process is partly involved in the observed reduction of neointima. Although the mobilization of EPC might be considered unfavorable for tumor growth, multiple clinical trials have recommended the use of Epo in chemotherapy-associated anemia or for longer survival among patients with multiple myeloma.[30] Thus, the safety and feasibility of Epo treatment has been established. Although it was a concern that erythropoiesis may increase the risk of thrombosis because of an elevation in blood viscosity or cause hypertension resulting from the induction of the vasoconstricting hormone endothelin-1,[31] thrombosis formation at the injured lesion in the Epo-treated group was similar to the saline-injected group, and blood pressure did not increase after short-term Epo-treatment (unpublished observation, 2005). Moreover, Epo was reported to attenuate cytokine production and inflammation in tissue ischemia by targeting cell apoptosis[32] or to induce cellular protection by activating Epo-EpoR signals involving Akt pathways,[33] consistent with the present result (Figure 6). These antiinflammatory and antiapoptotic cytoprotection actions associated with endothelial EpoR-mediated Akt/NO signaling may also contribute to the preventive effect of Epo on the neointimal hyperplasia.

EPC-like cells were reportedly derived from more differentiated $CD34^+$ or immature $CD133^+$ hematopoietic stem cells, as well as from PB MNCs or $CD14^+$ monocytes.[2,8,16] These EPC-like cells lose CD45 hematopoietic markers and express endothelial markers. Our present study clearly showed that $CD45^{dim}/Flk\text{-}1^+$ or $Sca1^+/Flk\text{-}1^+$ EPCs were mobilized by Epo, had a functional EC-like property in vitro, and contributed to endothelial regeneration after wire-mediated injury, suggesting this cell type is an EPC-like cell responsible for Epo-induced vascular repair. Thus, Epo treatment may be a novel strategy to inhibit the neointimal hyperplasia by directly acting on the injured vessels as well as mobilizing EPCs to the neoendothelium.

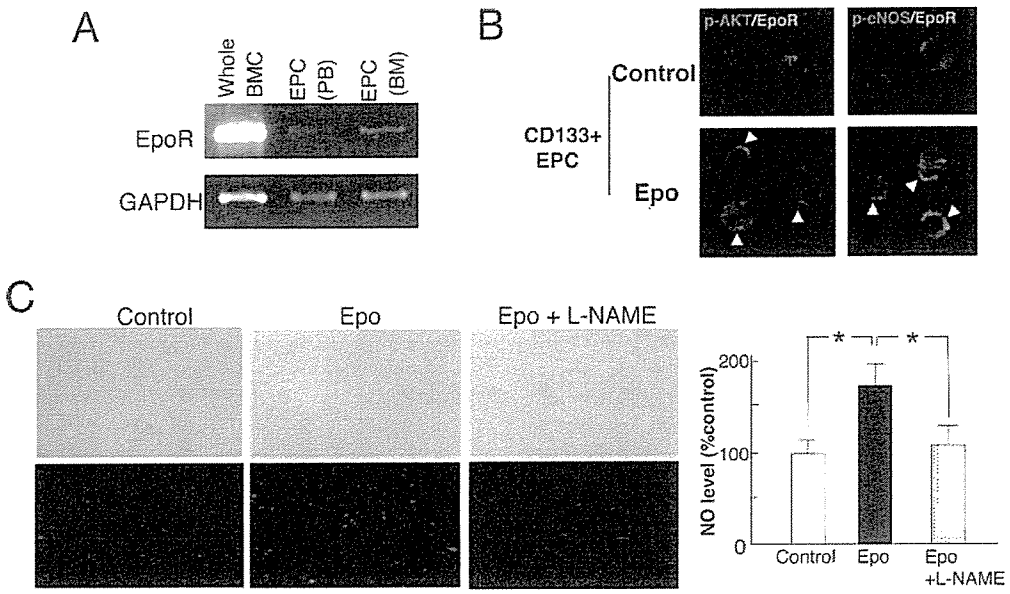

Figure 6. Epo-mediated activation of Akt/eNOS and NO production in PB-derived endothelial progenitor cells. A, The Sca1$^+$/Flk-1$^+$ EPCs were isolated from the PB and BM by FACS. Total RNAs were prepared from them and the whole BM cells and subsequently subjected to RT-PCR analysis using the primers for EpoR and GAPDH. The DNA fragments corresponding to EpoR and GAPDH were amplified in the predicted sizes. B, CD133$^+$ progenitor cells were purified to >90% purity from human PB MNCs by positive selection using anti-CD133$^+$ microbeads and a magnetic cell sorting device and then were primary cultured. After 12 hours of serum starvation (0.5% serum), they were stimulated by 1.2 IU/mL Epo for 30 minutes and immunostained for EpoR (green) with phosphorylated Akt kinase (red) or phosphorylated eNOS (red) (bar=25 μm). Double-fluorescence–positive cells appear yellow (arrowheads). C, Measurement of the intracellular NO level. The CD133$^+$ cells were loaded with DAF-FM DA (10 μmol/L), and NO was visualized as a green dot under laser microscopy. The averaged intensity in the Epo and the Epo plus L-NAME cells relative to the control group was evaluated. $^*P<0.005$ (n=8, each).

Acknowledgments

This work was supported by a Grant from the Ministry of Education, Culture, Science and Technology of Japan.

References

1. Libby P, Schwartz D, Brogi E, Tanaka H, Clinton SK. A cascade model for restenosis. A special case of atherosclerosis progression. *Circulation.* 1992;86(suppl III):III-47–III-52.
2. Asahara T, Murohara T, Sullivan A, Silver M, van der Zee R, Li T, Witzenbichler B, Schatteman G, Isner JM. Isolation of putative progenitor endothelial cells for angiogenesis. *Science.* 1997;275:964–967.
3. Asahara T, Masuda H, Takahashi T, Kalka C, Pastore C, Silver M, Kearne M, Magner M, Isner JM. Bone marrow origin of endothelial progenitor cells responsible for postnatal vasculogenesis in physiological and pathological neovascularization. *Circ Res.* 1999;85:221–228.
4. Griese DP, Ehsan A, Melo LG, Kong D, Zhang L, Mann MJ, Pratt RE, Mulligan RC, Dzau VJ. Isolation and transplantation of autologous circulating endothelial cells into denuded vessels and prosthetic grafts: implications for cell-based vascular therapy. *Circulation.* 2003;108: 2710–2715.
5. Fujiyama S, Amano K, Uehira K, Yoshida M, Nishiwaki Y, Nozawa Y, Jin D, Takai S, Miyazaki M, Egashira K, Imada T, Iwasaka T, Matsubara H. Bone marrow monocyte lineage cells adhere on injured endothelium in a monocyte chemoattractant protein-1-dependent manner and accelerate reendothelialization as endothelial progenitor cells. *Circ Res.* 2003;93: 980–989.
6. Werner N, Junk S, Laufs U, Link A, Walenta K, Bohm M, Nickenig G. Intravenous transfusion of endothelial progenitor cells reduces neointima formation after vascular injury. *Circ Res.* 2003;93:e17–e24.
7. Kong D, Melo LG, Mangi AA, Zhang L, Lopez-Ilasaca M, Perrella MA, Liew CC, Pratt RE, Dzau VJ. Enhanced inhibition of neointimal hyperplasia by genetically engineered endothelial progenitor cells. *Circulation.* 2004a;109:1769–1775.
8. Gulati R, Jevremovic D, Peterson TE, Witt TA, Kleppe LS, Mueske CS, Lerman A, Vile RG, Simari RD. Autologous culture-modified mononuclear cells confer vascular protection after arterial injury. *Circulation.* 2003;108:1520–1526.
9. Anagnostou A, Liu Z, Steiner M, Chin K, Lee ES, Kessimian N, Noguchi CT. Erythropoietin receptor mRNA expression in human endothelial cells. *Proc Natl Acad Sci U S A.* 1994;91:3974–3978.
10. Anagnostou A, Lee ES, Kessimian N, Levinson R, Steiner M. Erythropoietin has a mitogenic and positive chemotactic effect on endothelial cells. *Proc Natl Acad Sci U S A.* 1990;87:5978–5982.
11. Carlini RG, Alonzo EJ, Dominguez J, Blanca I, Weisinger JR, Rothstein M, Bellorin-Font E. Effect of recombinant human erythropoietin on endothelial cell apoptosis. *Kidney Int.* 1999;55:546–553.
12. Beleslin-Cokic BB, Cokic VP, Yu X, Weksler BB, Schechter AN, Noguchi CT. Erythropoietin and hypoxia stimulate erythropoietin receptor and nitric oxide production by endothelial cells. *Blood.* 2004; 103:921–926.
13. Heeschen C, Aicher A, Lehmann R, Fichtlscherer S, Vasa M, Urbich C, Mildner-Rihm C, Martin H, Zeiher AM, Dimmeler S. Erythropoietin is a potent physiologic stimulus for endothelial progenitor cell mobilization. *Blood.* 2003;102:1340–1346.
14. Ribatti D, Presta M, Vacca A, Ria R, Giuliani R, Dell'Era P, Nico B, Roncali L, Dammacco F. Human erythropoietin induces a pro-angiogenic phenotype in cultured endothelial cells and stimulates neovascularization in vivo. *Blood.* 1999;93:2627–2636.
15. Galeano M, Altavilla D, Cucinotta D, Russo GT, Calo M, Bitto A, Marini H, Marini R, Adamo EB, Seminara P, Minutoli L, Torre V, Squadrito F. Recombinant human erythropoietin stimulates angiogenesis and wound healing in the genetically diabetic mouse. *Diabetes.* 2004;53:2509–2517.
16. Kalka C, Masuda H, Takahashi T, Gordon R, Tepper O, Gravereaux E, Pieczek A, Iwaguro H, Hayashi SI, Isner JM, Asahara T. Vascular endothelial growth factor165 gene transfer augments circulating endothelial progenitor cells in human subjects. *Circ Res.* 2000;86:1198–1202.
17. Kocher AA, Schuster MD, Szabolcs MJ, Takuma S, Burkhoff D, Wang J, Homma S, Edwards NM, Itescu S. Neovascularization of ischemic myocardium by human bone-marrow-derived angioblasts prevents cardiomyocyte apoptosis, reduces remodeling and improves cardiac function. *Nat Med.* 2001;7:430–436.
18. Kong D, Melo LG, Gnecchi M, Zhang L, Mostoslavsky G, Liew CC, Pratt RE, Dzau VJ. Cytokine-induced mobilization of circulating endothelial progenitor cells enhances repair of injured arteries. *Circulation.* 2004b;110:2039–2046.

19. Sata M, Saiura A, Kunisato A, Tojo A, Okada S, Tokuhisa T, Hirai H, Makuuchi M, Hirata Y, Nagai R. Hematopoietic stem cells differentiate into vascular cells that participate in the pathogenesis of atherosclerosis. *Nat Med.* 2002;8:403–409.
20. Okabe M, Ikawa M, Kominami K, Nakanishi T, Nishimune Y. 'Green mice' as a source of ubiquitous green cells. *FEBS Lett.* 1997;407:313–319.
21. Zambrowicz BP, Imamoto A, Fiering S, Herzenberg LA, Kerr WG, Soriano P. Disruption of overlapping transcripts in the ROSA beta geo 26 gene trap strain leads to widespread expression of beta-galactosidase in mouse embryos and hematopoietic cells. *Proc Natl Acad Sci U S A.* 1997;94:3789–3794.
22. Hori T, Matsubara T, Ishibashi T, Yamazoe M, Ida T, Higuchi K, Takemoto M, Ochiai S, Tamura Y, Aizawa Y, Nishio M. Decrease of nitric oxide end-products during coronary circulation reflects elevated basal coronary artery tone in patients with vasospastic angina. *Jpn Heart J.* 2000;41:583–595.
23. Urbich C, Heeschen C, Aicher A, Sasaki K, Bruhl T, Farhadi MR, Vajkoczy P, Hofmann WK, Peters C, Pennacchio LA, Abolmaali ND, Chavakis E, Reinheckel T, Zeiher AM, Dimmeler S. Relevance of monocytic features for neovascularization capacity of circulating endothelial progenitor cells. *Circulation.* 2003;108:2511–2516.
24. Moroi M, Zhang L, Yasuda T, Virmani R, Gold HK, Fishman MC, Huang PL. Interaction of genetic deficiency of endothelial nitric oxide, gender, and pregnancy in vascular response to injury in mice. *J Clin Invest.* 1998;101:1225–1232.
25. Sata M, Maejima Y, Adachi F, Fukino K, Saiura A, Sugiura S, Aoyagi T, Imai Y, Kurihara H, Kimura K, Omata M, Makuuchi M, Hirata Y, Nagai R. A mouse model of vascular injury that induces rapid onset of medial cell apoptosis followed by reproducible neointimal hyperplasia. *J Mol Cell Cardiol.* 2000;32:2097–2104.
26. Beohar N, Flaherty JD, Davidson CJ, Maynard RC, Robbins JD, Shah AP, Choi JW, MacDonald LA, Jorgensen JP, Pinto JV, Chandra S, Klaus HM, Wang NC, Harris KR, Decker R, Bonow RO. Antirestenotic effects of a locally delivered caspase inhibitor in a balloon injury model. *Circulation.* 2004;109:108–113.
27. Hill JM, Syed MA, Arai AE, Powell TM, Paul JD, Zalos G, Read EJ, Khuu HM, Leitman SF, Horne M, Csako G, Dunbar CE, Waclawiw MA, Cannon RO 3rd. Outcomes and risks of granulocyte colony-stimulating factor in patients with coronary artery disease. *J Am Coll Cardiol.* 2005; 46:1643–1648.
28. Fukumoto Y, Miyamoto T, Okamura T, Inaba S, Harada M, Niho Y. Angina pectoris occurring during granulocyte colony-stimulating factor-combined preparatory regimen for autologous peripheral blood stem cell transplantation in a patient with acute myelogenous leukaemia. *Br J Haematol.* 1997;97:666–668.
29. Kawachi Y, Watanabe A, Kurooka N, Setsu K. Acute arterial thrombosis due to platelet aggregation in a patient receiving granulocyte colony-stimulating factor. *Br J Haematol.* 1996;94:413–416.
30. Rizzo JD, Lichtin AE, Woolf SH, Seidenfeld J, Bennett CL, Regan DH, Browman GP, Gordon MS; American Society of Clinical Oncology; American Society of Hematology. Use of epoetin in patients with cancer: evidence-based clinical practice guidelines of the American Society of Clinical Oncology and the American Society of Hematology. *Blood.* 2002;100:2303–2320.
31. Vogel V, Kramer HJ, Backer A, Meyer-Lehnert H, Jelkmann W, Fandrey J. Effects of erythropoietin on endothelin-1 synthesis and the cellular calcium messenger system in vascular endothelial cells. *Am J Hypertens.* 1997;10:289–296.
32. Genc S, Koroglu TF, Genc K. Erythropoietin as a novel neuroprotectant. *Res Neurol Neurosci.* 2004;22:105–119.
33. Chong ZZ, Kang JQ, Maiese K. Erythropoietin is a novel vascular protectant through activation of Akt1 and mitochondrial modulation of cysteine proteases. *Circulation.* 2002;106:2973–2979.

Available online at www.sciencedirect.com
SCIENCE DIRECT
Journal of Molecular and Cellular Cardiology 40 (2006) 510–519
Journal of Molecular and Cellular Cardiology
www.elsevier.com/locate/yjmcc

Original article

Nicorandil regulates Bcl-2 family proteins and protects cardiac myocytes against hypoxia-induced apoptosis

Susumu Nishikawa [a], Tetsuya Tatsumi [a,*], Jun Shiraishi [a], Shinsaku Matsunaga [a], Mitsuo Takeda [a], Akiko Mano [a], Miyuki Kobara [b], Natsuya Keira [a], Mitsuhiko Okigaki [a], Tomosaburo Takahashi [a], Hiroaki Matsubara [a]

[a] *Department of Cardiology and Vascular Regenerative Medicine, Kyoto Prefectural University of Medicine, Kyoto, Kawaramachi-Hirokoji, Kamigyo-ku, Kyoto 602-8566, Japan*
[b] *Department of Clinical Pharmacology, Kyoto Pharmaceutical University, Kyoto, Japan*

Received 12 August 2005; received in revised form 19 December 2005; accepted 24 January 2006

Abstract

Nicorandil has been shown to inhibit myocyte apoptosis by opening of mitochondrial ATP-sensitive potassium (mitoK_{ATP}) channels and nitrate-like effect against oxidative stress. However, the detailed mechanism of nicorandil-mediated cardioprotection under hypoxic conditions remains to be largely unknown. The present study examined whether nicorandil can inhibit apoptosis via regulation of Bcl-2 family proteins in hypoxic myocytes. Neonatal rat cardiac myocytes were exposed to hypoxia for 7 hours. Hypoxia-induced myocyte apoptosis (13.9 ± 0.9%) under glucose-rich conditions. Myocyte apoptosis was accompanied by loss of mitochondrial membrane potential ($\Delta\psi_m$), cytochrome *c* release from mitochondria into cytosol, and activation of caspase-3. Hypoxia also significantly increased Bax and decreased Bcl-2 mRNA and protein expression, thereby increasing Bax/Bcl-2 ratio. Nicorandil 100 μmol/l significantly decreased the percentage of apoptotic myocytes (7.2 ± 0.5%) by inhibiting loss of $\Delta\psi_m$ and translocation of cytochrome *c*. These effects of nicorandil were partially but significantly inhibited by cotreatment of either 500 μmol/l 5-hydroxydecanoate, a selective mitoK_{ATP} channel antagonist, or 10 μmol/l 1*H*-[1,2,4]oxidazolo[4,3-a]quinoxalin-1-one (ODQ), an inhibitor of soluble guanylate cyclase. Moreover, nicorandil significantly inhibited the hypoxia-induced changes in Bax and Bcl-2 expression, and concomitant increased Bax and decreased Bcl-2 immunoreactivity in mitochondria. These effects of nicorandil in Bax and Bcl-2 expression were significantly blunted by cotreatment of ODQ and 5-HD, respectively. Cotreatment of KT5823, an inhibitor of protein kinase G, significantly blocked the effect of nicorandil on Bax expression and 8-bromo-cyclic guanosine 3′,5′ monophosphate (8-bromo-cGMP), a cGMP analog, mimicked the effect of nicorandil on Bax expression. The present study demonstrates that nicorandil regulates Bcl-2 family proteins via opening of mitoK_{ATP} channels and nitric oxide-cGMP signaling and inhibits hypoxia-induced mitochondrial death pathway.

Keywords: Nicorandil; K_{ATP} channel; Hypoxia; Apoptosis; Bax; Bcl-2

1. Introduction

The anti-anginal agent nicorandil is an opener of ATP-sensitive potassium (K_{ATP}) channels with a nitrate moiety. An increasing body of evidence has demonstrated that nicorandil protects hearts against ischemic injury. For example, nicorandil can improve the recovery of postischemic contractile dysfunction and can reduce infarct size in several animal models [1,2] and in humans [3–6]. Recently, the impact of nicorandil in angina (IONA), a randomized and placebo-controlled study, has shown that nicorandil reduced the incidence of major cardiovascular events in patients with angina pectoris [7]. Although it still remains uncertain whether nicorandil has an infarct limiting effect in humans, a great deal of attention has been attracted by molecular mechanism by which nicorandil exerts cardioprotective action. Besides the beneficial hemodynamic effects such as increased coronary blood flow and reduced vascular resistance, recent studies have suggested that cardioprotective effects of nicorandil are mediated by activation of mitochondrial K_{ATP} (mitoK_{ATP}) channels in myocytes [8,9].

Myocardial ischemia is well documented to trigger cardiac cell death which possesses the properties of both apoptosis and necrosis [10,11]. Although apoptosis and necrosis were consid-

* Corresponding author. Tel.: +81 75 251 5511; fax: +81 75 251 5514.
E-mail address: tatsumi@koto.kpu-m.ac.jp (T. Tatsumi).

0022-2828/$ - see front matter © 2006 Elsevier Ltd. All rights reserved.
doi:10.1016/j.yjmcc.2006.01.020

ered to be conceptually and morphologically distinct forms of cell death, recent our and other reports have indicated that these two processes share common mitochondrial death signaling pathway, and that intracellular ATP levels are an important determinant in the regulation of myocyte death [12–16]. We further demonstrated that hypoxia increased expression of Bax, a proapoptotic protein, in the myocytes, and that translocation of cytosolic Bax into mitochondria is an important trigger to the loss of mitochondrial membrane potential ($\Delta\psi_m$), with a concomitant release of mitochondrial cytochrome *c* into cytosol [15,16]. In contrast, Bcl-2, a representative antiapoptotic protein, is demonstrated to prevent cytochrome *c* release and mediates antiapoptotic effects [17,18]. Apoptosis is thus governed by families of Bcl-2 proteins with positive and negative regulatory members, acting at serial steps along a programmed pathway [19]. Previous observations indeed indicated that Bcl-2 and Bax play an important pathophysiological role in the protection or acceleration of apoptosis in human myocytes after ischemia and/or reperfusion [20].

Several lines of evidence suggests that opening of mitoK$_{ATP}$ channels elicits preservation of mitochondrial integrity and consequent protection of cellular function [21], and that nitric oxide (NO) inhibits apoptosis through regulating Bcl-2 family proteins [22,23]. Although nicorandil has been demonstrated to inhibit oxidative stress-induced myocyte apoptosis via either opening of mitoK$_{ATP}$ channels or NO/cGMP-dependent pathway [21,24], it still remains largely unknown whether nicorandil can affect Bcl-2 family proteins in hypoxic myocytes. The present study was therefore designed to examine whether nicorandil can regulate the expression of Bax and Bcl-2 proteins, which play a crucial role in the regulation of mitochondrial permeability, and inhibit mitochondria-mediated death pathway in hypoxic myocytes.

2. Materials and methods

2.1. Cultured neonatal cardiac myocytes

Primary cultures of neonatal rat cardiac myocytes were prepared from neonatal Wistar rat hearts by digestion with 0.2% collagenase as described in [25]. Myocyte-rich fraction (separated by Percoll gradient) was resuspended in Dulbecco's modified Eagle's medium (DMEM) supplemented with 10% fetal bovine serum (FBS) [26]. Myocytes were cultured by bromodeoxyuridine (BrdU 10^{-4} mol/l) during the first 48 hours, and were then incubated in DMEM containing 0.5% FBS without BrdU. All experiments were performed 36–48 hours after this incubation.

2.2. Experimental protocols

Cell cultures were washed twice with phosphate buffer saline (PBS), followed by a final incubation in serum-deprived medium. During this final incubation, cardiac myocytes were treated with one of the following: 1) nicorandil (10–100 μmol/l), 2) nicorandil (100 μmol/l) in the presence of 2–20 μmol/l 1H-[1,2,4]oxidazolo[4,3-a]quinoxalin-1-one (ODQ), an inhibitor of soluble guanylate cyclase, 3) nicorandil (100 μmol/l) in the presence of 100–1000 μmol/l 5-hydroxydecanoate (5-HD), a selective mitoK$_{ATP}$ channel antagonist, 4) nicorandil (100 μmol/l) in the presence of 10 μg/ml cycloheximide (CHX), an inhibitor of protein synthesis, 5) nicorandil (100 μmol/l) in the presence of 1 μmol/l KT5823, an inhibitor of protein kinase G (PKG), 6) 1 mmol/l 8-bromo-cyclic guanosine 3′,5′ monophosphate (8-bromo-cGMP), a cGMP analog, 7) 100 μmol/l diazoxide, another selective mitoK$_{ATP}$ channel opener, or 8) diazoxide (100 μmol/l) in the presence of 500 μmol/l 5-HD. The myocytes were then transferred to a 37° C humidified chamber (F-102, Iijima Electronics Co., Aichi, Japan) which was flushed with 5% CO_2 and 95% nitrogen (less than 1% oxygen) for 7 hours as previously described in [25]. Diazoxide was applied only for 20 min before myocytes were exposed to hypoxia. Unless indicated otherwise, cells were exposed to those drugs during the entire experimental period. Control myocytes were incubated in serum-free DMEM for 7 hours under normoxia. According to our previous observation that intracellular ATP levels are an important determinant in the regulation of myocyte necrosis and apoptosis [15], we changed the glucose concentrations in the hypoxic medium to 100 mg/dl for evaluation of myocyte apoptosis.

2.3. Determination of myocyte apoptosis

Histochemical staining of myocyte was performed as previously described in [15,16,26]. The cells were visualized by fluorescein microscopy, and the images were generated by dual-exposure photography. Apoptotic cells were identified on the basis of distinctive condensed or fragmented nuclear morphology and apoptotic cell counts were expressed as a percentage of the total number of nuclei counted [15,16,26].

2.4. Mitochondrial membrane potential

Loss of $\Delta\psi_m$ was assessed by Dye JC-1 (Molecular Probes, Eugene, OR) [12]. Cells grown on coverslips were incubated in PBS containing 10^{-5} mol/l JC-1 at 37 °C for 5 min. Fluorescence emission at 527 and 590 nm was determined after excitation at 480 nm. The intensity of red fluorescence appearing in the mitochondria was quantitatively measured by NIH image.

2.5. Immunoblotting

For detection of cytochrome *c*, Bax, and Bcl-2, myocyte cell fractions (mitochondrial fraction and cytosolic fraction) were subjected to electrophoresis and blotting as described previously in [15–17,26]. The blots were reacted with antibodies for cytochrome *c* (7H8.2C12, PharMingen), Bax (PharMingen), Bcl-2 (PharMingen), followed by horseradish peroxidase (HRP)-conjugated anti-mouse IgG or HRP-conjugated anti-rabbit IgG (Amersham). Samples containing equal amounts of protein were transferred to a polyvinylidene difluoride membrane (Bio-Rad). Chemioluminescence was detected with ECL Western blot detection kits (Amersham) according to the supplier's recommendations.

2.6. Caspase-3 activity

Caspase-3 enzymatic activity was determined with a CPP32 assay kit (MBL, Japan), which detects the production of the chromophore *p*-nitroanilide after its cleavage from the peptide substrate DEVD-*p*-nitroanilide, as described previously in [27].

2.7. Real-time polymerase chain reaction

Total RNA (1 μg) was reverse transcribed with Super Script III First-Strand-Synthesis System (Invitrogen). First-Strand cDNA was assessed by CYBR Green I real-time polymerase chain reaction (PCR) (LightCycler, Roche). Specific oligonucleotide primer sequences were as follows. For Bax, sense: 5′-ACCCTGTGAGCGGACATC-3′; anti-sense: 5′-CTAGTAGT GACAAGTAGGG-3′. For Bcl-2, sense: 5′-GATACTGGA GATGAAGACTC-3′; anti-sense: 5′-TGCAGCTGACTGGA CATC-3′. For β-actin, sense: 5′-GTGGGGCGCCCCAGGCAC CA-3′; anti-sense: 5′-CTCCTTATTGTCACGCACGATTTC-3′. After initial denaturation at 95 °C for 10 min, reactions were cycled 40 times using following parameters for Bax and Bcl-2 detection: 95 °C for 0 s, primer annealing at 55 °C for 5 s, and primer extension at 72 °C for 10 s. The expressions of Bax and Bcl-2 were normalized to the expression levels of β-actin.

2.8. Statistical analysis

Data are expressed as mean ± S.E.M. of at least six samples derived from more than six separate experiments. Differences were analyzed by one-way analysis of variance combined with the Fisher post-hoc test. A P-value of < 0.05 was considered to indicate statistical significance.

3. Results

3.1. Effect of nicorandil on hypoxia-induced apoptosis

Histochemical nuclear staining with Hoechst 33258, and immunohistochemical staining of cellular desmin revealed apopto-

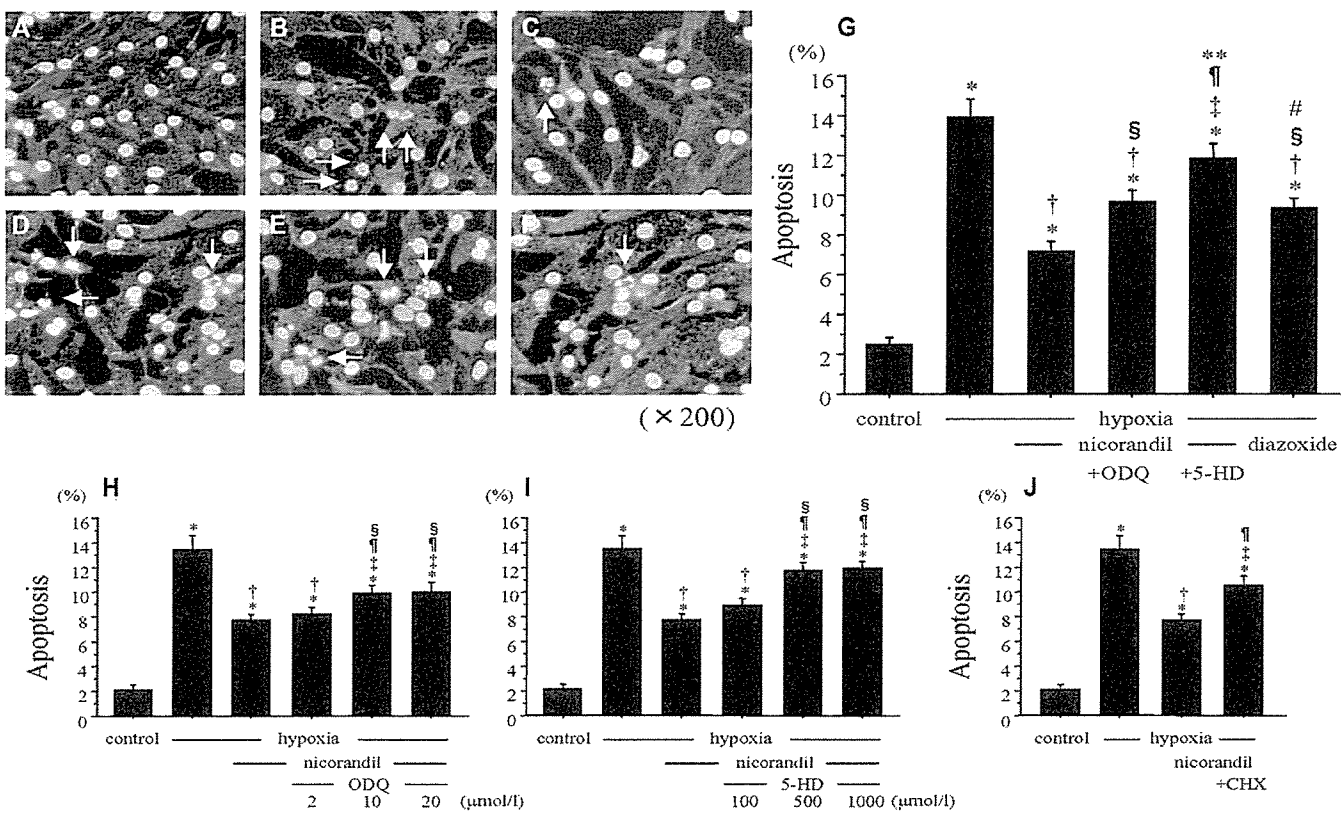

Fig. 1. Histochemical characterization of apoptotic myocytes. Myocytes were treated with and nicorandil (100 μmol/l) alone, nicorandil (100 μmol/l) in the presence of 2–20 μmol/l ODQ, nicorandil (100 μmol/l) in the presence of 100–1000 μmol/l 5-HD, 100 μmol/l diazoxide, or nicorandil (100 μmol/l) in the presence of 10 μg/ml CHX, and then were exposed to hypoxia for 7 hours in serum-free DMEM containing 100 mg/dl glucose. Control myocytes were incubated in serum-free DMEM for 7 hours under normoxia. The myocytes were then stained with an anti-desmin polyclonal antibody and Hoechst 33258. Representative micrographs show myocytes maintained under normoxic conditions (A, control), and myocytes following 7 hours hypoxia (B), following 7 hours hypoxia with nicorandil (C), following 7 hours hypoxia with nicorandil with 10 μmol/l ODQ (D), following 7 hours hypoxia with nicorandil with 500 μmol/l 5-HD (E), following 7 hours hypoxia pretreated with diazoxide (F), respectively (magnification ×200). Arrows indicate the typical feature of apoptotic myocytes. (G–J) Percentage of apoptotic myocytes. Myocyte apoptosis was calculated as described in Section 2 ($n = 6$). (G) $*P < 0.0001$ vs. control; $\dagger P < 0.0001$, $\ddagger P < 0.05$ vs. hypoxia; $\P P < 0.0001$, $\S P < 0.01$ vs. nicorandil; $**P < 0.05$ vs. nicorandil with 10 μmol/l ODQ; $\#P < 0.01$ vs. nicorandil with 500 μmol/l 5-HD. (H) $*P < 0.0001$ vs. control; $\dagger P < 0.0001$, $\ddagger P < 0.001$ vs. hypoxia; $\P P < 0.05$ vs. nicorandil, $\S P < 0.05$ vs. nicorandil with 2 μmol/l ODQ. (I) $*P < 0.0001$ vs. control; $\dagger P < 0.0001$, $\ddagger P < 0.05$ vs. hypoxia; $\P P < 0.0001$ vs. nicorandil, $\S P < 0.001$ vs. nicorandil with 100 μmol/l 5-HD. (J) $*P < 0.0001$ vs. control; $\dagger P < 0.0001$, $\ddagger P < 0.01$ vs. hypoxia; $\P P < 0.01$ vs. nicorandil.

tic myocytes with typical fragmented nuclei and condensed chromatin 7 hours after hypoxia, as illustrated in Fig. 1. The percentage of apoptotic myocytes increased to 13.9 ± 0.9% after 7 hours hypoxia, as compared with control (2.5 ± 0.3%). Nicorandil (10–100 μmol/l) inhibited myocyte apoptosis in a dose-dependent fashion (data not shown), such that 100 μmol/l nicorandil significantly reduced the percentage of apoptotic cells to 7.2 ± 0.5%. The antiapoptotic effect of 100 μmol/l nicorandil was inhibited by either cotreatment of ODQ (2–20 μmol/l) or 5-HD (100–1000 μmol/l) in a dose-dependent fashion, while ODQ (20 μmol/l) or 5-HD (1000 μmol/l) did not further affect the action of nicorandil to apoptosis any more. Thus, the antiapoptotic effect of 100 μmol/l nicorandil was significantly inhibited by either cotreatment of 10 μmol/l ODQ (9.7 ± 0.6%) or 500 μmol/l 5-HD (11.9 ± 0.7%). Moreover, this antiapoptotic effect of nicorandil was significantly inhibited by cotreatment of 10 μg/ml CHX, an inhibitor of protein synthesis (10.5 ± 0.7%). The percentage of myocyte apoptosis was also assessed by fluorescence-activated cell sorter analysis, as previously described in [26], and ascertained that the percentage of apoptosis was compatible with that estimated by Hoechst 33258 staining (data not shown).

Diazoxide (100 μmol/l) also significantly inhibited myocyte apoptosis after 7 hours hypoxia, although the antiapoptotic effects were smaller than that of nicorandil under our experimental conditions (Fig. 1).

3.2. Mitochondrial membrane potential

JC-1, potentially a sensitive mitochondrial probe, can be used to monitor $\Delta\psi_m$ in apoptotic myocytes [28]. Control myocytes showed red–orange mitochondrial staining, indicative of normal high membrane potentials. In contrast, after 7 hours hypoxia, myocytes showed green fluorescence, indicating loss of $\Delta\psi_m$ (Fig. 2). Quantitative analysis of red fluorescence showed that hypoxia significantly decreased $\Delta\psi_m$ to 17.2 ± 3.1%, and that both nicorandil and diazoxide inhibited the hypoxia-induced loss of $\Delta\psi_m$ to 75.6 ± 3.5% and 70.0 ± 3.4%, respectively. The effect of nicorandil on $\Delta\psi_m$ was also partially but significantly blunted by cotreatment of ODQ or 5-HD to 50.0 ± 4.5% and 27.8 ± 3.3%, respectively.

3.3. Cytochrome c release

Fig. 3 illustrates the effects of 7 hours hypoxia on the intracellular localization of cytochrome *c* in the myocytes. Prior to hypoxia, cytochrome *c* was detected exclusively in the mitochondrial fraction. Hypoxia caused a modest decline in cytochrome *c* immunoreactivity in the mitochondrial fraction, with a concomitant increase in the cytosolic fraction, reaching 404.0 ± 20.8% of control. Nicorandil significantly suppressed the hypoxia-induced immunoreactivity of cytochrome *c* in the cytosolic fraction to 179.8 ± 26.9%. Moreover, cotreatment of

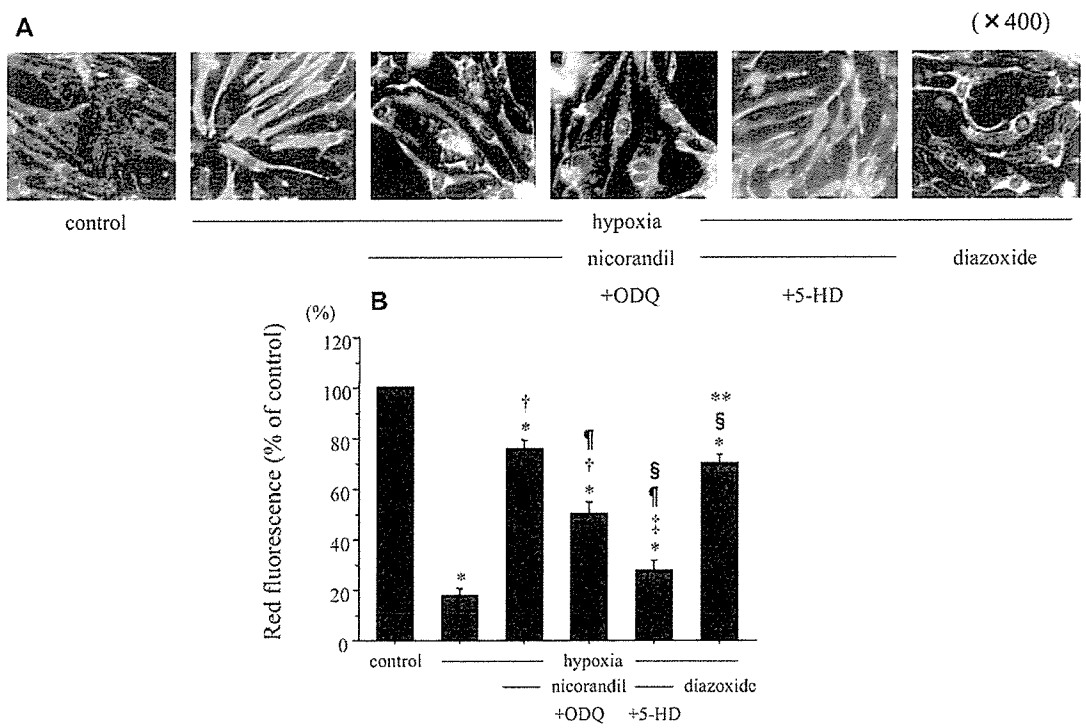

Fig. 2. Loss of mitochondrial membrane potential ($\Delta\psi_m$). Myocytes were treated with and nicorandil (100 μmol/l) alone, nicorandil (100 μmol/l) in the presence of 10 μmol/l ODQ, nicorandil (100 μmol/l) in the presence of 500 μmol/l 5-HD, or 100 μmol/l diazoxide, and then were exposed to hypoxia for 7 hours in serum-free DMEM containing 100 mg/dl glucose. Control myocytes were incubated in serum-free DMEM for 7 hours under normoxia. (A) Loss of $\Delta\psi_m$ was assessed by Dye JC-1, as described in Section 2 (magnification × 400). (B) Quantitative analysis of red fluorescence. Levels of red fluorescence are shown as a percentage of change in the mean values from six independent experiments compared with serum-deprived control. *$P < 0.0001$ vs. control; †$P < 0.0001$, ‡$P < 0.05$ vs. hypoxia; ¶$P < 0.0001$ vs. nicorandil; §$P < 0.0001$ vs. nicorandil with ODQ; **$P < 0.0001$ vs. nicorandil with 5-HD.

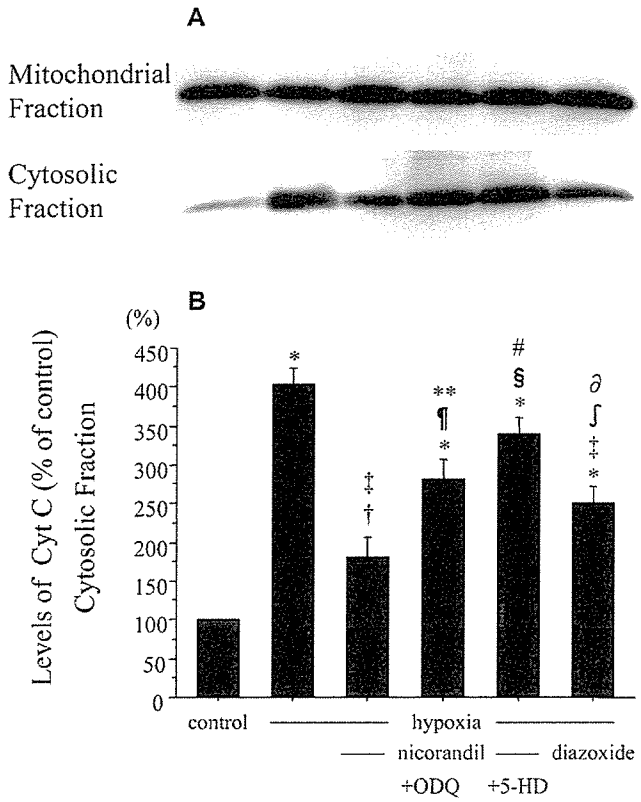

Fig. 3. Western blot analysis of translocation of cytochrome *c* (Cyt C) from mitochondria into cytosol. Myocytes were treated according to the protocol described in the legend of Fig. 2. (A) Mitochondrial and cytosolic fractions (20 μg protein) were probed with antibody for cytochrome *c*. Representative immunoblots are shown from three independent experiments. (B) Densitometric analysis of cytochrome *c* release. Levels of cytochrome *c* are shown as a percentage of change in the mean values from three independent experiments compared with serum-deprived control. $*P < 0.0001$, $\dagger P < 0.05$ vs. control; $\ddagger P < 0.0001$, $\P P < 0.001$, $\S P < 0.05$ vs. hypoxia; $**P < 0.01$, $\#P < 0.0001$ $\int P < 0.05$ vs. nicorandil; $\partial P < 0.01$ vs. nicorandil with 5-HD.

ODQ or 5-HD with nicorandil significantly increased cytochrome *c* immunoreactivity in the cytosolic fraction to 281.0 ± 25.6% and 338.8 ± 22.7%, respectively. Diazoxide also attenuated the hypoxia-induced immunoreactivity of cytochrome *c* in the cytosolic fraction to 250.5 ± 21.7%, although the effect was smaller than that of nicorandil.

3.4. Caspase-3 activity

Caspase-3 activity in the myocytes exposed to 7 hours hypoxia was significantly increased by 3.2 ± 0.2 fold, as compared with control (Fig. 4). Nicorandil significantly inhibited the hypoxia-induced activation of caspase-3 to 1.9 ± 0.2 fold of control. Cotreatment of ODQ or 5-HD with nicorandil partially but significantly increased caspase-3 activity to 2.3 ± 0.1 and 2.8 ± 0.2 fold, respectively. Diazoxide also blunted the hypoxia-induced activation of caspase-3 to 2.4 ± 0.1 fold, although the effect was smaller than that of nicorandil.

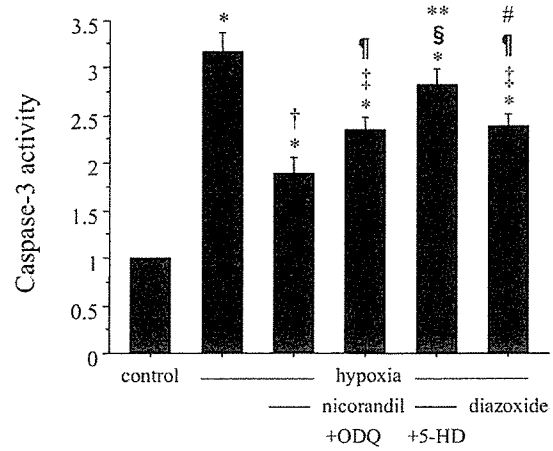

Fig. 4. Caspase-3 activity in myocytes. Myocytes were treated according to the protocol described in the legend of Fig. 2. Caspase-3 activity was determined as described in Section 2. Activation level of caspase-3 is shown as a percentage of change in mean value of six samples derived from at least three separate experiments. $*P < 0.0001$ vs. control; $\dagger P < 0.0001$, $\ddagger P < 0.001$ vs. hypoxia; $\P P < 0.05$, $\S P < 0.0001$ vs. nicorandil; $**P < 0.05$ vs. nicorandil with ODQ; # $P < 0.05$ vs. nicorandil with 5-HD.

3.5. Regulation of Bcl-2 family proteins

Fig. 5 illustrated Bax expression in the cytosolic and mitochondrial fractions. Hypoxia significantly increased Bax immunoreactivity to 181.0 ± 15.9% of control in the cytosolic fraction and enhanced Bax translocation into the mitochondrial fraction to 170.3 ± 12.7%. Nicorandil significantly inhibited the hypoxia-induced incline in Bax in the cytosolic and mitochondrial fractions to 98.7 ± 13.1% and 100.3 ± 13.2%, respectively. Cotreatment of ODQ with nicorandil partially but significantly increased Bax in the cytosolic and mitochondrial fractions to 153.3 ± 13.4% and 143.7 ± 15.2%, respectively. In contrast, cotreatment of 5-HD with nicorandil did not affect Bax. Diazoxide also did not significantly affect Bax immunoreactivity in the cytosolic and mitochondrial fractions.

In addition, cotreatment of KT5823 with nicorandil significantly increased Bax in the cytosolic and mitochondrial fractions to 172.0 ± 6.5% and 164.0 ± 5.7%, respectively. In contrast, 8-bromo-cGMP significantly attenuated Bax immunoreactivity in the cytosolic and mitochondrial fractions to 115.0 ± 8.4% and 109.5 ± 9.3%, respectively (Fig. 6). The increment ratio between cytosolic and mitochondrial fraction of Bax was not significantly changed by hypoxia and/or pharmacological treatment (data not shown).

Bcl-2 was detected only in the mitochondrial fraction. Hypoxia significantly decreased Bcl-2 immunoreactivity to 35.3 ± 5.0% of control (Fig. 7). Nicorandil significantly inhibited the hypoxia-induced decline in Bcl-2 to 79.3 ± 6.6%. Cotreatment of ODQ with nicorandil did not affect Bcl-2. In contrast, cotreatment of 5-HD with nicorandil partially but significantly decreased Bcl-2 to 49.7 ± 7.0%. Diazoxide also significantly blunted the hypoxia-induced decline in Bcl-2 immunoreactivity

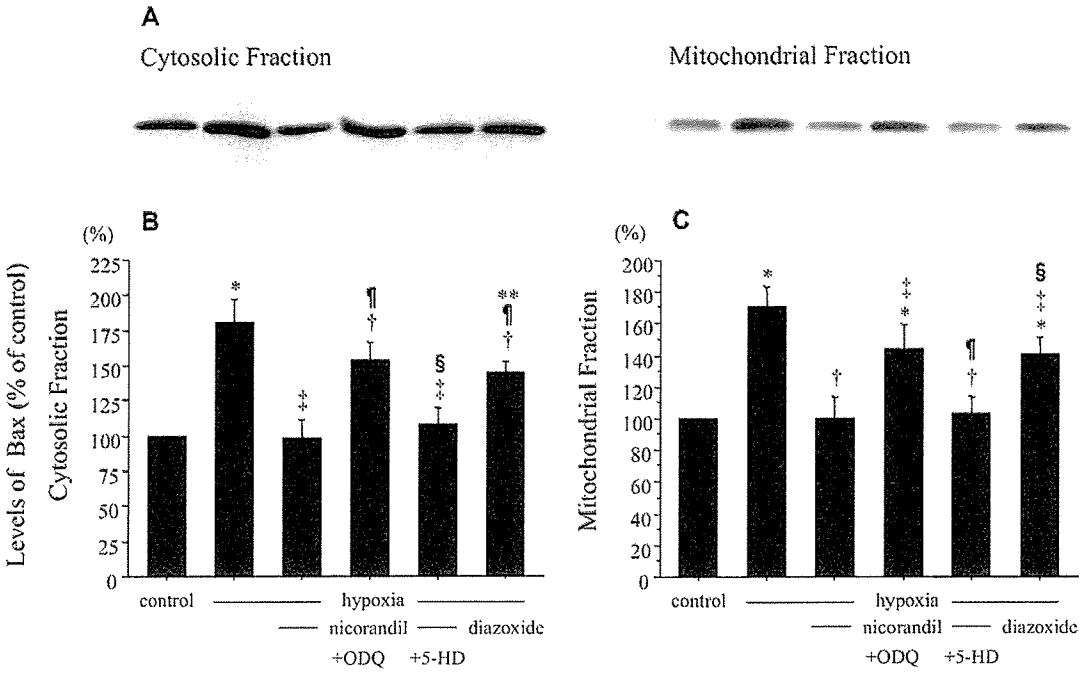

Fig. 5. Western blot analysis of Bax expression. Myocytes were treated according to the protocol described in the legend of Fig. 2. Cell extracts (20 μg protein) were probed with anti-Bax antibodies. (A) Immunoblots shown are representative from three independent experiments. (B, C) Densitometric analysis of Bax expression in cytosol and translocation into mitochondria. Levels of Bax are shown as a percentage of change in the mean value derived from three independent experiments. (B) $*P < 0.001$, $\dagger P < 0.01$ vs. control; $\ddagger P < 0.001$ vs. hypoxia; $\P P < 0.01$ vs. nicorandil; $\S P < 0.05$ vs. nicorandil with ODQ; $**P < 0.05$ vs. nicorandil with 5HD. (C) $*P < 0.05$ vs. control; $\dagger P < 0.01$ vs. hypoxia; $\ddagger P < 0.05$ vs. nicorandil; $\P P < 0.05$ vs. nicorandil with ODQ; $\S P < 0.05$ vs. nicorandil with 5-HD.

to 79.3 ± 7.0%. Moreover, the effect of diazoxide on Bcl-2 immunoreactivity was significantly inhibited by 5-HD (Fig. 7).

The mRNA expression levels of Bax and Bcl-2 analyzed by real-time RT-PCR were shown in Fig. 8. Hypoxia significantly increased Bax mRNA expression to 2.5 ± 0.2 fold of control and decreased Bcl-2 mRNA expression to 0.4 ± 0.1 fold of control. Nicorandil significantly inhibited hypoxia-induced incline in Bax mRNA to 1.3 ± 0.1 fold and decline in Bcl-2 mRNA to 0.8 ± 0.1 fold. Moreover, cotreatment of ODQ with nicorandil did not affect Bcl-2 mRNA expression but significantly increased Bax mRNA expression to 2.3 ± 0.2 fold. In contrast, cotreatment of 5-HD with nicorandil did not affect Bax mRNA expression but significantly decreased Bcl-2 mRNA expression to 0.5 ± 0.1 fold. Diazoxide did not affect Bax mRNA expression but significantly inhibited hypoxia-induced decline in Bcl-2 mRNA to 0.8 ± 0.1 fold.

4. Discussion

The present study has shown that hypoxia significantly increased the relative expression of Bax/Bcl-2 in mitochondria and induced loss of $\Delta\psi_m$, cytochrome *c* release from mitochondrial into cytosol, and activation of caspase-3, which were involved in the common pathway of necrotic and apoptotic death in the myocytes. Nicorandil inhibited this death signaling cascade through not only opening of mitoK$_{ATP}$ channels but also nitrate-like effect, since the effects were significantly inhibited by cotreatment of either 5-HD or ODQ. Furthermore, our data demonstrate for the first time that 1) nicorandil inhibits the hypoxia-induced Bax overexpression and concomitantly accelerated translocation of Bax into mitochondria from cytosol via NO-cGMP signaling, and 2) nicorandil upregulates the mitochondrial Bcl-2 expression reduced by hypoxia via opening of mitoK$_{ATP}$ channels in hypoxic myocytes. The data therefore suggest that cardioprotective effects of nicorandil work either in the mitochondrial membranes or in the upstream of mitochondrial death signaling pathway.

Nicorandil is an opener of K$_{ATP}$ channels with a nitrate moiety. Although it was initially assumed that cardioprotection by nicorandil is attributable to the reduction of preload and afterload, the observation that a mitoK$_{ATP}$ channel-selective agent diazoxide was similarly protective against myocardial injury focused attention on mitoK$_{ATP}$ channels [29]. We have previously reported that hypoxia accelerates mitochondria-mediated common cascade to myocyte necrosis and apoptosis in an ATP-dependent fashion [15]. In the present study, hypoxic myocytes resulted in morphologically characterized changes to apoptosis with induction of loss of $\Delta\psi_m$, and activation of caspase-3 following release of cytochrome *c* from mitochondria into cytosol, in consistent with our previous data [15]. We also observed that hypoxia-induced myocyte necrosis (54.4 ± 3.2%) under glucose-free conditions, and that nicorandil (10–100 μmol/l) inhibited myocyte necrosis in a dose-dependent fashion (data not shown). Thus, nicorandil significantly inhibited the hypoxia-induced both cell demises, suggesting that this agent acts mitochondria-mediated intrinsic

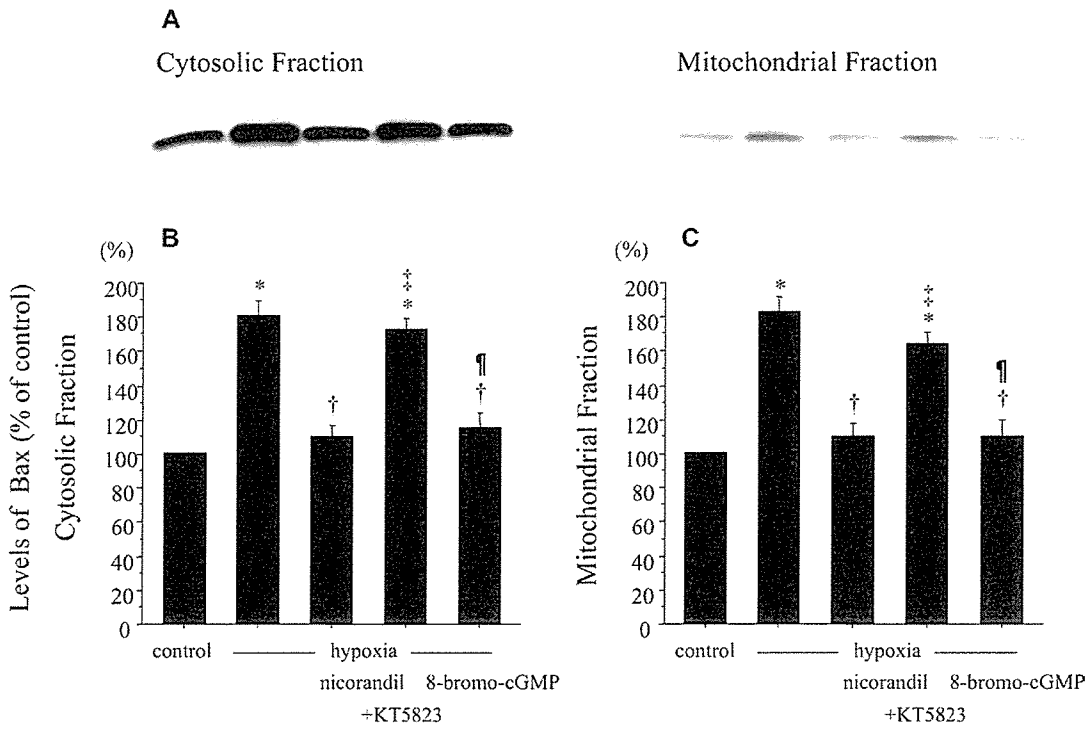

Fig. 6. Western blot analysis of Bax expression. Myocytes were treated with and nicorandil (100 μmol/l) alone, nicorandil (100 μmol/l) in the presence of 1 μmol/l KT5823, or 1 mmol/l 8-bromo-cyclic guanosine 3′,5′ monophosphate (8-bromo-cGMP), and then were exposed to hypoxia for 7 hours in serum-free DMEM containing 100 mg/dl glucose. Control myocytes were incubated in serum-free DMEM for 7 hours under normoxia. Cell extracts (20 μg protein) were probed with anti-Bax antibodies. (A) Immunoblots shown are representative from three independent experiments. (B) Densitometric analysis of Bax expression in cytosol and translocation into mitochondria. Levels of Bax are shown as a percentage of change in the mean value derived from three independent experiments. $*P < 0.0001$, vs. control; $\dagger P < 0.0001$ vs. hypoxia; $\ddagger P < 0.0001$ vs. nicorandil; $\P P < 0.0001$ vs. nicorandil with KT5823.

death signaling pathway via mitoK$_{ATP}$ channels, rather than receptor-mediated extrinsic pathway.

Mitochondrial K$_{ATP}$ channels are thought to play a key role in cardioprotection, as previous studies reported that opening of mitoK$_{ATP}$ channels mimic ischemic preconditioning [30] and inhibit myocyte apoptosis [31]. Since the antiapoptotic effect of nicorandil was significantly inhibited by cotreatment of CHX, our data suggest that the cardioprotective effect of nicorandil is relevant with second-window protection. To explain the cardioprotection by nicorandil, one important action to activate mitoK$_{ATP}$ channels has been described in a prior experimental study [8]. By opening of mitoK$_{ATP}$ channels, nicorandil is demonstrated to depolarize the mitochondrial membrane and attenuate mitochondrial matrix Ca^{2+} overload triggered by ischemia/hypoxia or oxidative stress [32]. Indeed, our results show that either nicorandil or diazoxide significantly inhibited the hypoxia-induced loss of $\Delta\psi_m$, which effect of nicorandil was partially inhibited by cotreatment of 5-HD. As another important cardioprotective action, nitrate moiety of nicorandil is proposed to inhibit apoptosis by either cGMP-dependent mechanism or sulfhydryl modification of caspase-3 activity [24]. Our results show that inhibitory effect of nicorandil on the hypoxia-induced mitochondrial death cascade was partially but significantly blunted by cotreatment of ODQ, in consistent with the previous data [24]. Thus, it seems likely that nicorandil exerts cardioprotection cooperatively via mitoK$_{ATP}$ channels and cGMP accumulation, however, the detailed mechanisms by which exist in the upstream of mitochondrial disruption remain still elusive.

Bcl-2 family proteins can be divided into antiapoptotic members (e.g. Bcl-2 and Bcl-xL) and proapoptotic members (e.g. Bax, Bak, Bid, Bad, Bim, Noxa, Puma, and BNip3, etc.) [33]. Bax, a representative multidomain proapoptotic Bcl-2 family protein, controls access of upstream apoptotic signals to mitochondria [34]. Bax is held in an inactive state in cytosol by the insertion of its most C-terminal α-helix into a hydrophobic cleft created by its BH1-3 domains [35]. In response to apoptotic stimuli such as ischemia/hypoxia, this helix is presumed to move out of the cleft causing a conformational change. These events are considered to trigger Bax translocation into mitochondria, oligomerization, and insertion into the outer mitochondrial membrane via its C-terminal α-helix. In this study, hypoxia significantly increased Bax mRNA and protein expression, and nicorandil significantly inhibited the hypoxia-induced Bax overexpression and concomitant incline in Bax immunoreactivity in mitochondria. Since cotreatment of ODQ but not 5-HD with nicorandil partially but significantly increased Bax immunoreactivity in hypoxic myocytes, cotreatment of KT5823 with nicorandil significantly increased Bax immunoreactivity, and 8-bromo-cGMP mimicked the effect of nicoran-

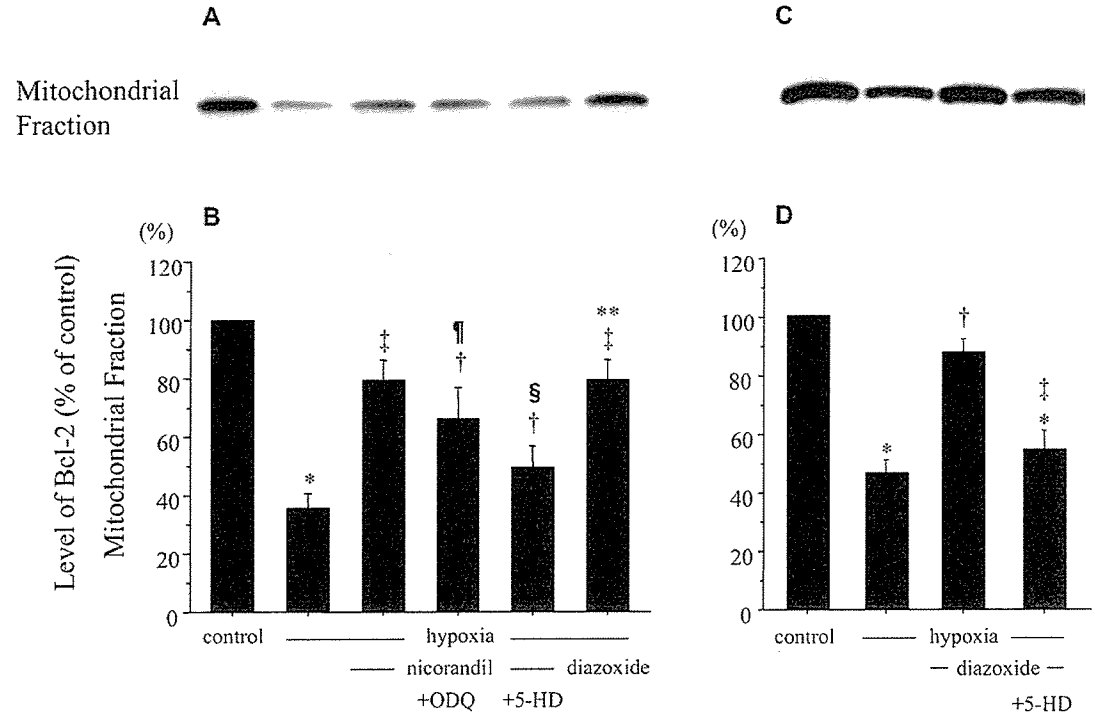

Fig. 7. Western blot analysis of Bcl-2 expression. Myocytes were treated according to the protocol described in the legend of Fig. 2 and diazoxide (100 μmol/l) in the presence of 500 μmol/l 5-HD. Cell extracts (20 μg protein) were probed with anti-Bcl-2 antibodies. (A, C) Immunoblots shown are representative from three independent experiments. (B, D) Densitometric analysis of Bcl-2 expression in the mitochondria. Levels of Bcl-2 are shown as a percentage of change in the mean value derived from three independent experiments. (B) $*P < 0.0001$, $\dagger P < 0.01$vs. control; $\ddagger P < 0.001$, $\P P < 0.01$ vs. hypoxia; $\S P < 0.01$ vs. nicorandil; $**P < 0.01$ vs. nicorandil with 5-HD. (D) $*P < 0.0001$, vs. control; $\dagger P < 0.0001$ vs. hypoxia; $\ddagger P < 0.001$ vs. diazoxide.

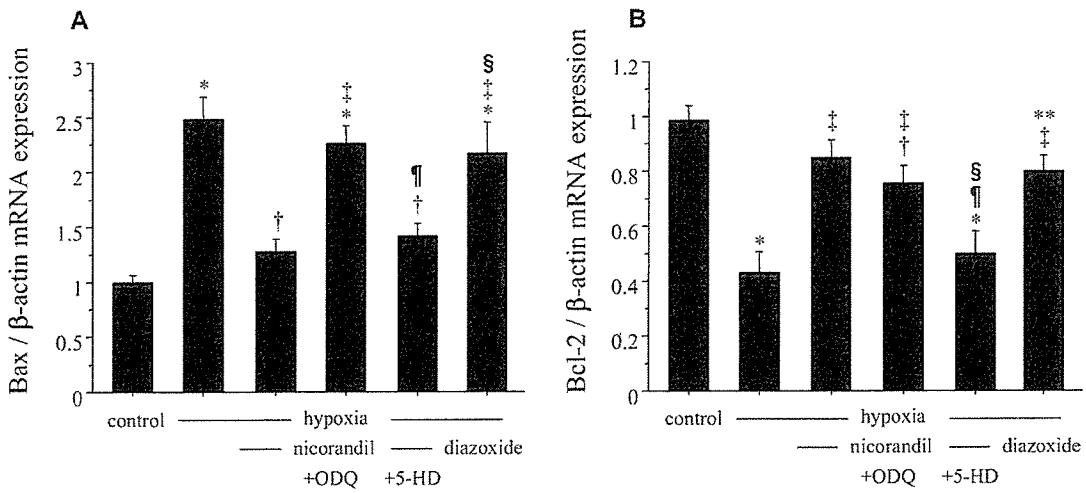

Fig. 8. Real-time RT-PCR analysis of Bax and Bcl-2 mRNA expressions. Myocytes were treated according to the protocol described in the legend of Fig. 2. Real-time RT-PCR was performed to determine Bax (A) and Bcl-2 (B) mRNA levels, and was normalized to β-actin expression. RT-PCR analysis shown is representative from three independent experiments. Levels of mRNA are expressed relative to control myocytes in the mean values derived from three independent experiments. (A) $*P < 0.0001$ vs. control; $\dagger P < 0.001$ vs. hypoxia; $\ddagger P < 0.001$ vs. nicorandil; $\P P < 0.01$ vs. nicorandil with ODQ; $\S P < 0.01$ vs. nicorandil with 5-HD. (B) $*P < 0.0001$, $\dagger P < 0.05$ vs. control; $\ddagger P < 0.001$ vs. hypoxia; $\P P < 0.001$ vs. nicorandil; $\S P < 0.05$ vs. nicorandil with ODQ; $**P < 0.01$ vs. nicorandil with 5-HD.

dil on Bax, it is considered that cGMP and/or PKG play a crucial role in the regulation of Bax expression in hypoxic myocytes.

Bcl-2, an antiapoptotic family member, is constitutively localized at the outer mitochondrial membrane and it is known to antagonize multidomain and BH3-only proapoptotic Bcl-2 family proteins. The present study shows that hypoxia significantly decreased expression of Bcl-2 mRNA and protein in mitochondria, and that nicorandil significantly inhibited the hypoxia-induced decline in Bcl-2 expression. Since cotreatment of 5-HD but not ODQ with nicorandil partially but significantly attenuated Bcl-2 expression in hypoxic myocytes, it

seems likely that opening of mitoK$_{ATP}$ channels by nicorandil maintained mitochondrial Bcl-2 expression. Moreover, since Bcl-2 protein has been demonstrated to inhibit deterioration of $\Delta\psi_m$ in in vitro assay [36], nicorandil is possible to contribute to maintenance of $\Delta\psi_m$ by regulating Bcl-2 expression through opening of mitoK$_{ATP}$ channels. On the other hand, Cheng and Kirsch et al. [37,38] reported that Bcl-2 is cleaved at Asp-34 by caspase-3 and suggested that there exists a positive feedback loop between Bcl-2 and caspases for executing apoptosis. Taken together, Bcl-2 family proteins may be complicatedly regulated by several key factors, including cGMP and/or PKG, mitoK$_{ATP}$ channels, and caspases. The ratio of Bcl-2 or Bcl-xL to Bax or Bak was previously reported to determine whether the cell lives or dies [39]. In contrast, other data raise the possibility that previously demonstrated interactions between these proteins may be an artifact of the nonionic detergents in the buffers used [40]. In this study, the ratio of Bax/Bcl-2 under hypoxic conditions was increased by 5.0 ± 0.8 fold, as compared with control. Nicorandil significantly decreased the ratio to 1.3 ± 0.2 fold. Cotreatment of ODQ and 5-HD with nicorandil partially tended to decrease the ratio to 2.3 ± 0.4 fold and 2.1 ± 0.1 fold, respectively. Our data thus suggest that nicorandil decreases the relative expression of Bax/Bcl-2 in mitochondria and protects hypoxic myocytes, although the implication of the ratio is still under controversial. Moreover, recent reports suggest that Bax directly causes an increase in mitochondrial outer membrane permeability that releases cytochrome *c* to mediate caspase activation independent of mitochondrial permeability transition, and that loss of cytochrome *c* may have a secondary effect to cause loss of $\Delta\psi_m$ [41,42]. The effects of nicorandil on Bax and Bcl-2 may act independently for cell survival through mitochondrial permeability, although further investigation will be necessary to fully clarify molecular mechanisms by which nicorandil exerts cardioprotective effect against hypoxic injury.

In conclusion, the present study demonstrates for the first time that nicorandil can regulate the Bax and Bcl-2 proteins in mitochondria and suppresses mitochondrial death pathway through opening of mitoK$_{ATP}$ channels and NO-cGMP signaling pathway in hypoxic myocytes, a fact which may have significant implications in the development of future therapies to combat the effects of myocardial ischemia.

References

[1] Mizunuma T, Nithipaticom K, Gross GJ. Effects of nicorandil and glyceryl trinitrate on infarct size, adenosine release, and neutrophil infiltration in the dog. Cardiovasc Res 1995;29:482–9.

[2] Imagawa J, Baxter GF, Yellon DM. Myocardial protection afforded by nicorandil and ischemic preconditioning in a rabbit infarct model in vivo. J Cardiovasc Pharmacol 1998;31:74–9.

[3] Saito S, Mizumura T, Takayama T, Honye J, Fukui T, Kamata T, et al. Antiischemic effects of nicorandil during coronary angioplasty in humans. Cardiovasc Drugs Ther 1995;9:257–63.

[4] Kobayashi Y, Goto Y, Daikoku S, Itoh A, Miyazaki S, Ohshima S, et al. Cardioprotective effect of intravenous nicorandil in patients with successful reperfusion for acute myocardial infarction. Jpn Circ J 1998;62:183–9.

[5] Ito H, Taniyama Y, Iwakura K, Nishikawa N, Masuyama T, Kuzuya T, et al. Intravenous nicorandil can preserve microvascular integrity and myocardial viability in patients with reperfused anterior wall myocardial infarction. J Am Coll Cardiol 1999;33:654–60.

[6] Patel DJ, Purcell HJ, Fox KM. Cardioprotection by opening of the K_{ATP} channel in unstable angina: is this a clinical manifestation of myocardial preconditioning? Results of a randomized study with nicorandil. CESAR 2 investigation. Clinical European studies in angina and revascularization. Eur Heart J 1999;20:51–7.

[7] The IONA Study Group. Effect of nicorandil on coronary events in patients with stable angina: the impact of nicorandil in angina (IONA) randomized trial. Lancet 2002;359:1269–75.

[8] Sato T, Sasaki N, O'Rourke B, Marban E. Nicorandil, a potent cardioprotective agent, acts by opening mitochondrial ATP-dependent potassium channels. J Am Coll Cardiol 2000;35:514–8.

[9] Hachida M, Lu H, Ohkado A, Gu H, Zhang XL, Furukawa H, et al. Effect of ATP-potassium channel opener nicorandil on long-term cardiac preservation. J Cardiovasc Surg (Torino) 2000;41:533–9.

[10] Bialik S, Geenen DL, Sasson IE, Cheng R, Horner JW, Evans SM, et al. Myocyte apoptosis during acute myocardial infarction in the mouse localizes to hypoxic regions but occurs independently of p53. J Clin Invest 1997;100:1363–72.

[11] Kajstura J, Cheng W, Reiss K, Clark WA, Sonnenblick EH, Krajewski S, et al. Apoptotic and necrotic myocyte cell deaths are independent contributing variables of infarct size in rats. Lab Invest 1996;74:86–107.

[12] Ankarcrona M, Dypbukt JM, Bonfoco E, Zhivotovsky B, Orrenius S, Lipton SA, et al. Glutamate-induced neuronal death: a succession of necrosis or apoptosis depending on mitochondrial function. Neuron 1995; 15:961–73.

[13] Leist M, Gantner F, Bohlinger I, Tiegs G, Germann PG, Wendel A. Tumor necrosis factor-induced hepatocyte apoptosis precedes liver failure in experimental murine shock models. Am J Pathol 1995;146:1220–34.

[14] Shimizu S, Eguchi Y, Kamiike W, Itoh Y, Hasegawa J, Yamabe K, et al. Induction of apoptosis as well as necrosis by hypoxia and predominant prevention of apoptosis by Bcl-2 and Bcl-xL. Cancer Res 1996;56:2161–6.

[15] Tatsumi T, Shiraishi J, Keira N, Akashi K, Mano A, Yamanaka S, et al. Intracellular ATP is required for mitochondrial apoptotic pathways in isolated hypoxic rat cardiac myocytes. Cardiovasc Res 2003;59:428–40.

[16] Shiraishi J, Tatsumi T, Keira N, Akashi K, Mano A, Yamanaka S, et al. Important role of energy-dependent mitochondrial pathways in cultured rat cardiac myocyte apoptosis. Am J Physiol Heart Circ Physiol 2001; 281:H1637–H1647.

[17] Yang J, Liu X, Bhalla K, Kim CN, Ibrado AM, Cai J, et al. Prevention of apoptosis by Bcl-2: release of cytochrome *c* from mitochondrial blocked. Science 1997;275:1129–32.

[18] Kluck RM, Bossy-Wetzel E, Green DR, Newmeyer DD. The release of cytochrome *c* from mitochondria; a primary site for Bcl-2 regulation of apoptosis. Science 1997;275:1132–6.

[19] Oltvani ZN, Korsmeyer SJ. Checkpoints of dueling dimers foli death wishes. Cell 1994;79:189–92 (Review).

[20] Misao J, Hayakawa Y, Ohno M, Kato S, Fujiwara T, Fujiwara H. Expression of bcl-2 protein, an inhibitor of apoptosis, and Bax, an accelerator of apoptosis, in ventricular myocytes of human hearts with myocardial infarction. Circulation 1996;94:1506–12.

[21] Akao M, Teshima Y, Marban E. Antiapoptotic effect of nicorandil mediated by mitochondorial ATP-sensitive potassium channels in cultured cardiac myocyte. J Am Coll Cardiol 2002;40:803–10.

[22] Genaro AM, Hortelano S, Alvarez A, Martinez C, Bosca L. Splenic B lymphocyte programmed cell death is prevented by nitric oxide release through mechanisms involving sustained Bcl-2 levels. J Clin Invest 1995;95:1884–90.

[23] Suschek CV, Krischel V, Bruch-Gerharz D, Berendji D, Krutmann J, Kroncke KD, et al. Nitric oxide fully protects against UVA-induced apoptosis in tight correlation with Bcl-2 up-regulation. J Biol Chem 1999;274:6130–7.

[24] Nagata K, Obata K, Odashima M, Yamada A, Somura F, Nishizawa T, et al. Nicorandil inhibits oxidative stress-induced apoptosis in cardiac myocytes through activation of mitochondrial ATP-sensitive potassium channels and a nitrate-like effect. J Mol Cell Cardiol 2003;35:1505–12.

[25] Matoba S, Tatsumi T, Keira N, Kawahara A, Akashi K, Kobara M, et al. Cardioprotective effect of angiotensin-converting enzyme inhibition against hypoxia/reoxygenation injury in cultured rat cardiac myocytes. Circulation 1999;99:817–22.
[26] Yamanaka S, Tatsumi T, Shiraishi J, Mano A, Keira N, Matoba S, et al. Amlodipine inhibits doxorubicin-induced apoptosis in neonatal rat cardiac myocytes. J Am Coll Cardiol 2003;41:870–8.
[27] Casciola-Rosen L, Nicholson DW, Chong T, Rowan KR, Thornberry NA, Miller DK, et al. Apopain/CPP32 cleaves proteins that are essential for cellular repair: a fundamental principle of apoptotic death. J Exp Med 1996;183:1957–64.
[28] Cook SA, Sugden PH, Clerk A. Regulation of bcl-2 proteins during development and in response to oxidative stress cardiac myocytes: association with changes in mitochondrial membrane potential. Circ Res 1999; 85:940–9.
[29] Gross GJ, Fryer RM. Sarcolemmal versus mitochondrial ATP-sensitive K + channels and myocardial preconditioning. Circ Res 1999;84:973–9.
[30] O'Rourke B. Myocardial K_{ATP} channels in preconditioning. Circ Res 2000;87:845–55.
[31] Akao M, Ohler A, O'Rourke B. Mitochondrial ATP-sensitive potassium channels inhibit apoptosis induced by oxidative stress in cardiac cells. Circ Res 2001;88:1267–75.
[32] Murata M, Akao M, O'Rourke B, Marban E. Mitochondrial ATP-sensitive potassium channels attenuate Matrix Ca^{2+} overload during simulated ischemia and reperfusion. Circ Res 2001;89:891–8.
[33] Crow MT, Mani K, Nam YJ, Kitsis RN. The mitochondrial death pathway and cardiac myocyte apoptosis. Circ Res 2004;95:957–70.
[34] Wei MC, Zong WX, Cheng EH, Lindsten T, Panoutsakopoulou V, Ross AJ, et al. Proapoptotic BAX and BAK: a requisite gateway to mitochodrial dysfunction and death. Science 2001;292:727–30.
[35] Suzuki M, Youle RJ, Tjandra N. Structure of Bax: coregulation of dimmer formation and intracellular localization. Cell 2000;103:645–54.
[36] Zamzami N, Susin SA, Marchetti P, Hirsch T, Gomez-Monterrey I, Castedo M, et al. Mitochondrial control of nuclear apoptosis. J Exp Med 1996;183:1533–44.
[37] Cheng E-Y, Kirsch DG, Clem RJ, Ravi R, Kastan MB, Bedi A, et al. Conversion of Bcl-2 to a Bax-like death effector by caspases. Science 1997;278:1966–8.
[38] Kirsch DG, Doseff A, Chau BN, Lim D-S, de Souza-Pinto NC, Hansford R, et al. Caspase-3-dependent cleavage of Bcl-2 promotes release of cytochrome *c*. J Biol Chem 1999;274:21155–61.
[39] Oltvai ZN, Milliman CL, Korsmeyer SJ. Bcl-2 heterodimerizes in vivo with a conserved homolog, Bax, that accelerates programmed cell death. Cell 1993;74:609–19.
[40] Hsu YT, Youle RJ. Nonionic detergents induce dimerization among members of the Bcl-2 family. J Biol Chem 1997;272:13829–34.
[41] Nakagawa T, Shimizu S, Watanabe T, Yamaguchi O, Otsu K, Yamagata H, et al. Cyclophilin D-dependent mitochondrial permeability transition regulates some necrotic but not apoptotic cell death. Nature 2005;434: 652–8.
[42] Baines CP, Kaiser RA, Purcell NH, Blair NS, Osinska H, Hambleton MA, et al. Loss of cyclophilin D reveals a critical role for mitochondrial permeability transition in cell death. Nature 2005;434: 658–62.